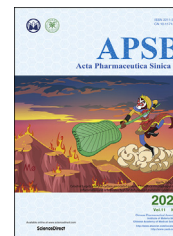




Chinese Pharmaceutical Association
Institute of Materia Medica, Chinese Academy of Medical Sciences

Acta Pharmaceutica Sinica B

www.elsevier.com/locate/apsb
www.sciencedirect.com



ORIGINAL ARTICLE

Design, synthesis, and biological evaluation of Bcr-Abl PROTACs to overcome T315I mutation



Liang Jiang^{a,†}, Yuting Wang^{a,†}, Qian Li^{a,†}, Zhengchao Tu^a,
Sihua Zhu^a, Sanfang Tu^{b,*}, Zhang Zhang^{a,*}, Ke Ding^{a,*},
Xiaoyun Lu^{a,*}

^aInternational Cooperative Laboratory of Traditional Chinese Medicine Modernization and Innovative Drug Development, Ministry of Education (MOE) of China, School of Pharmacy, Jinan University, Guangzhou 510632, China

^bDepartment of Hematology, Zhujiang Hospital, Southern Medical University, Guangzhou 510282, China

Received 27 June 2020; received in revised form 27 October 2020; accepted 2 November 2020

KEY WORDS

CML;
PROTAC;
Degradation;
T315I mutation;
Clinical resistance

Abstract Bcr-Abl threonine 315 to isoleucine 315 (T315I) gatekeeper mutation induced drug resistance remains an unmet clinical challenge for the treatment of chronic myeloid leukemia (CML). Chemical degradation of Bcr-Abl^{T315I} protein has become a potential strategy to overcome drug resistance. Herein, we first described the design, synthesis, and evaluation of a new class of selective Bcr-Abl^{T315I} proteolysis-targeting chimeric (PROTAC) degraders based on GZD824 (reported as Bcr-Abl^{T315I} inhibitor by our group). One of the degrader **7o** with 6-member carbon chain linkage with pomalidomide exhibits the most potent degradation efficacy with DR of 69.89% and 94.23% at 100 and 300 nmol/L, respectively, and has an IC₅₀ value of 26.8 ± 9.7 nmol/L against Ba/F3^{T315I} cells. Further, **7o** also displays substantial tumor regression against Ba/F3-Bcr-Abl^{T315I} xenograft model *in vivo*.

© 2021 Chinese Pharmaceutical Association and Institute of Materia Medica, Chinese Academy of Medical Sciences. Production and hosting by Elsevier B.V. This is an open access article under the CC BY-NC-ND license (<http://creativecommons.org/licenses/by-nc-nd/4.0/>).

Abbreviations: ALL, acute lymphoblastic leukemia; CML, chronic myeloid leukemia; cIAP1, cellular inhibitor of apoptosis protein 1; Co-IP, co-immunoprecipitation; CRBN, cereblon; DR, degradation rate; IC₅₀, cellular inhibition; TGI, tumor growth inhibition; LSCs, leukemic stem cells; PROTAC, proteolysis-targeting chimeric; NMPA, National Medical Products Administration; Ph⁺, Philadelphia chromosome; T315I, threonine 315 to isoleucine 315; VHL, von Hippel-Lindau.

*Corresponding authors. Tel.: +86 20 85223259.

E-mail addresses: doctortutu@163.com (Sanfang Tu), zhang_zhang@jnu.edu.cn (Zhang Zhang), dingke@jnu.edu.cn (Ke Ding), luxy2016@jnu.edu.cn (Xiaoyun Lu).

[†]These authors made equal contributions to this work.

Peer review under responsibility of Chinese Pharmaceutical Association and Institute of Materia Medica, Chinese Academy of Medical Sciences.

<https://doi.org/10.1016/j.apsb.2020.11.009>

2211-3835 © 2021 Chinese Pharmaceutical Association and Institute of Materia Medica, Chinese Academy of Medical Sciences. Production and hosting by Elsevier B.V. This is an open access article under the CC BY-NC-ND license (<http://creativecommons.org/licenses/by-nc-nd/4.0/>).

1. Introduction

Chronic myeloid leukemia (CML) is a hematological malignancy characterized by the occurrence of the Philadelphia chromosome (Ph⁺) and the resulting oncogenic *Bcr-Abl* gene^{1,2}. The Bcr-Abl inhibitor imatinib was the first approved drug for the conventional treatment of Ph⁺CML, also pioneering the era of kinase-targeted drug therapy. However, emerging acquired resistance to imatinib, commonly caused by point mutations in kinase domain of Abl, has become a major challenge for clinical management of CML^{3,4}. Subsequently, the second-generation Bcr-Abl inhibitors nilotinib, dasatinib and bosutinib have been approved for the treatment of CML patients with acquired resistance to imatinib^{5,6}. Unfortunately, all of them are not capable of inhibiting all of the imatinib resistant mutants, especially for the most notably Bcr-Abl threonine 315 to isoleucine 315 (T315I) gatekeeper mutation. Many efforts have been made to develop the third-generation Bcr-Abl inhibitors to overcome T315I mutation⁷. To date, ponatinib is the only approved 3rd Bcr-Abl inhibitor for the treatment of resistant CML and acute lymphoblastic leukemia (ALL) patients harboring T315I mutation^{8,9}.

Despite this, evidence of a dose-dependent increase in the risk of vascular occlusive events on ponatinib has limited its potential for a broader indication in CML¹⁰. Furthermore, sequential ponatinib treatment in patients can induce ~25% T315I-inclusive compound mutations (*e.g.*, E255K/T315I, T315I/F359C, etc.), which are insensitive to all Abl inhibitors including ponatinib^{11,12}. On the other hand, the hypothesized persistent leukemic stem cells (LSCs) explained by Bcr-Abl's scaffold protein function led to CML patients on lifelong small inhibitors treatment^{13,14}. Thus, it is suggested that chemical knockdown of Bcr-Abl^{T315I} may provide a promising potential therapeutic benefit for CML treatment.

The recent developed proteolysis-target chimeras (PROTACs) utilize hetero-bifunctional small molecules to achieve selective degradation of a target protein^{15,16}. Upon PROTACs binding a target protein and E3 ubiquitin ligase to form a ternary complex, the target protein is first ubiquitinated by E2 ligase, then subsequently degraded by 26S proteasome. Since the first androgen receptor (AR) PROTACs reported in 2008¹⁷, this technology has been successfully utilized for degradation of several targets, such as BRD4¹⁸ and ERR α ¹⁹, as well as many kinases²⁰. Comparing with traditional occupancy-driven inhibitors, PROTACs act catalytically and transiently to abolish biological function of a target protein with reduced drug exposure and toxicity as well as reduced resistant mutations^{15,21}. Thus, PROTACs have the potential advantage of overcoming the resistance of small molecule inhibitors.

Bcr-Abl wild type and T315I mutants selectively express in CML and AML cells, which provides an ideal target for PROTAC study without safety concern. The first series of Bcr-Abl PROTACs were reported based on dasatinib and bosutinib linkage either von Hippel-Lindau (VHL) or cereblon (CRBN) ligands from Crew's group (Fig. 1)²². The representative degrader **1** exhibited the degradation of c-Abl at 1 μ mol/L and was active against K562 cells with an EC₅₀ of 4.4 nmol/L. Subsequently, others PROTACs (**2–4**), designed based on imatinib, dasatinib and ABL001, respectively, were also reported to display significant degradation against Bcr-Abl^{23,24}. However, similar to the degrader **1**, there are no *in vivo* efficacious data to disclose to date. Most recently, Jiang et al.²⁵ disclosed a compound (**5**) with dasatinib linkage VHL as an Bcr-Abl degrader with promising *in vitro* and *in vivo* efficacies, as well as with efficacy against some clinical Bcr-Abl mutants, including G250E, V299L, F317L and

F317V (Fig. 1). However, this degrader is inactive to the clinically Bcr-Abl mutant carrying the T315I mutation. During this paper submission, Rao et al.²⁶ published a series of ponatinib-based Bcr-Abl degrader, which displaying the moderate degradation activity against Bcr-Abl^{T315I}. Herein we report our efforts to discover a new class of selective Bcr-Abl^{T315I} degraders based on our previous reported Bcr-Abl^{T315I} inhibitor GZD824 (**6**)²⁷.

2. Results and discussion

2.1. Design of Bcr-Abl^{T315I} degraders

We have identified GZD824 as a new orally bioavailable candidate with potency against a broad spectrum of Bcr-Abl mutants, including the gatekeeper T315I and the p-loop mutations (Fig. 2A)²⁷. GZD824 has been approved by the National Medical Products Administration (NMPA) for clinical trial study in 2015 and entered in phase II in 2018 (NCT03883087). The molecular docking indicated that GZD824 bound to the ATP binding pocket with type II mode, and the methylpiperazine group was exposed to solvent region, where was suitable for linkage an E3 ligase ligand for PROTACs design (Fig. 2B). From Fig. 1, it was suggested that three kinds of E3 ligases, *i.e.*, CRBN, VHL and cellular inhibitor of apoptosis protein 1 (cIAP1), and two kinds of linkers, *i.e.*, ethylenedioxy and carbon chains, have been utilized to design of Bcr-Abl PROTACs. Thus, we designed the PROTACs bifunctional compounds by tethering GZD824 with the aforementioned ligase ligands and linkers with different length to explore the degradation ability. In addition, an adamantyl group as “hydrophobic tag”, leading to a target misfolding and degradation by UPS²⁸, was also utilized to design the PROTACs.

2.2. Chemistry

The synthesis of title PROTACs is shown in Schemes 1–3. The synthetic route of the PMB protected POI ligand **18** is outlined in Scheme 1. Briefly, bromination of the starting material **8** gave bromide **9**, which was treated with *N*-Boc-piperazine under basic conditions and further reduction by Fe/NH₄Cl to yield the aniline **11**. Treatment of methyl 3-iodobenzoate **7** under palladium catalysis afforded the Sonogashira coupling product **13**, which was further coupled with PMB-protected 5-bromo-1*H*-pyrazolo [3,4-*b*]pyridine (**15**) to afford the alkyne **16**. Condensation with **11** and **16** gave the amide **18**²⁷. The synthesis of CRBN ligand conjugated linkers (**22a–22g**, **26** and **29a–29h**) and linker (**32**) are shown in Scheme 2. The various ethylenedioxy and ethylidene linkers were reacted with CRBN ligands (pomalidomide, lenalidomide and thalidomide) to afford the linkers **22a–22g**, **26** and **29a–29h**. The general synthetic routes of studied PROTACs are shown in Scheme 3. Compound **18** condensed with various CRBN linkers and further were deprotected by TFA to yield the corresponding PROTACs **7a–7c** and **7g–7s** (Scheme 3A). Further substitution of **18** with *tert*-butyl 3-(2-(2-(tosyloxy)ethoxy)ethoxy)propanoate **21b** gave the intermediate **30** and removal of the protecting group to afford **31**. Condensation of **31** with VHL ligand and amantadine afforded the PROTACs **7d** and **7f** (Scheme 3B). Moreover, a similar synthetic procedure with substitution and deprotection of **18**, and further condensation with CIAP ligand gave the PROTAC **7e** (Scheme 3C).

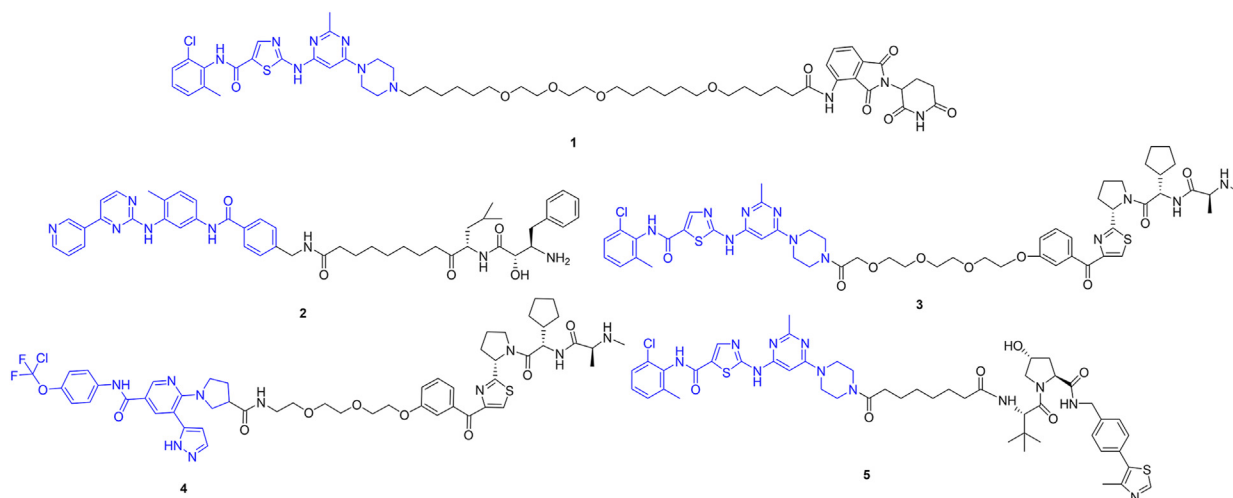


Figure 1 Previously reported Bcr-Abl PROTACs.

2.3. Structure degradation relationships

Since ethylenedioxy linker has ever been reported to be effective for Bcr-Abl PROTAC design^{22,29}, we first linked GZD824 to CRBN (pomalidomide, lenalidomide and thalidomide), VHL, cIAP1 E3 ligand and “hydrophobic tag” adamantyl group through 8-member (contain 2 PEG) length ethylenedioxy linker to afford PROTACs **7a–7f** (Table 1). The degradation efficiency of designed Bcr-Abl PROTACs was first evaluated in Ba/F3 cells expressed Bcr-Abl^{T315I} at 0, 33.3, 100 and 300 nmol/L with 24 h treatment. It was found that only compound **7a**, in which

pomalidomide possessing a CO (carbonyl group) linkage to ethylenedioxy, demonstrated moderate degradation potential for Bcr-Abl^{T315I} at 300 nmol/L with degradation rate (DR) of 39.01%, 2-fold potency than GZD824 (Table 1, Supporting Information Fig. S1). While compound **7a** does not exhibit obvious degradation on K562 cells expressing Bcr-Abl with the treatment of 24 h (data not shown). Further antiproliferative activities of **7a–7f** against CML cell lines K562, Ba/F3 Bcr-Abl^{WT} and Ba/F3 Bcr-Abl^{T315I} were performed with the CCK-8 assay. The results also showed that the compound **7a** has the strongest antiproliferative activity against Ba/F3^{T315I} cell lines, which is corresponding to

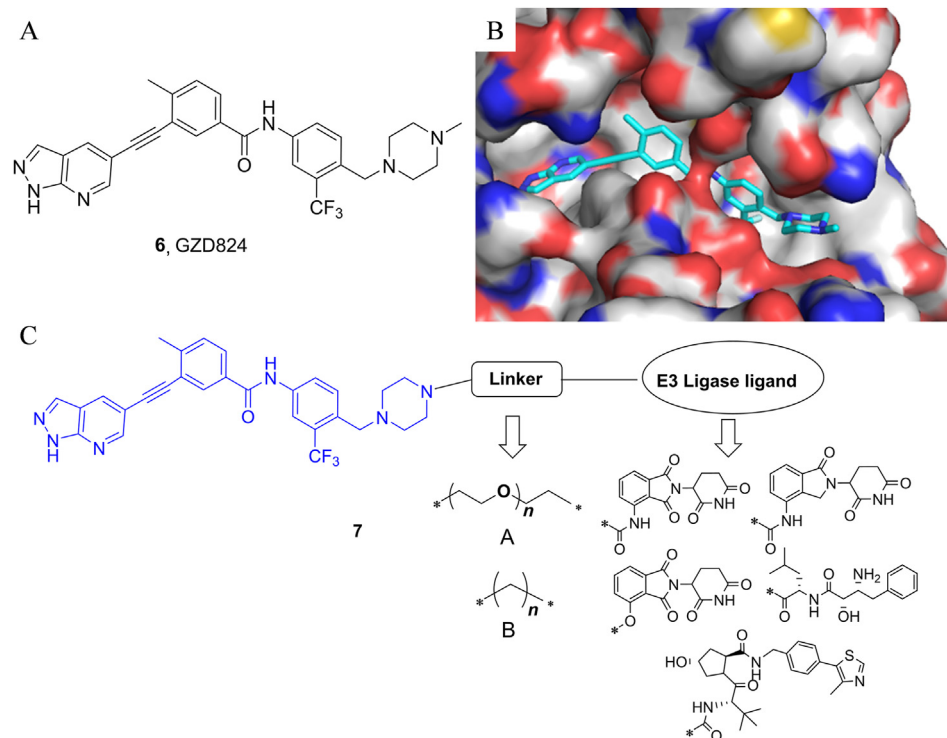
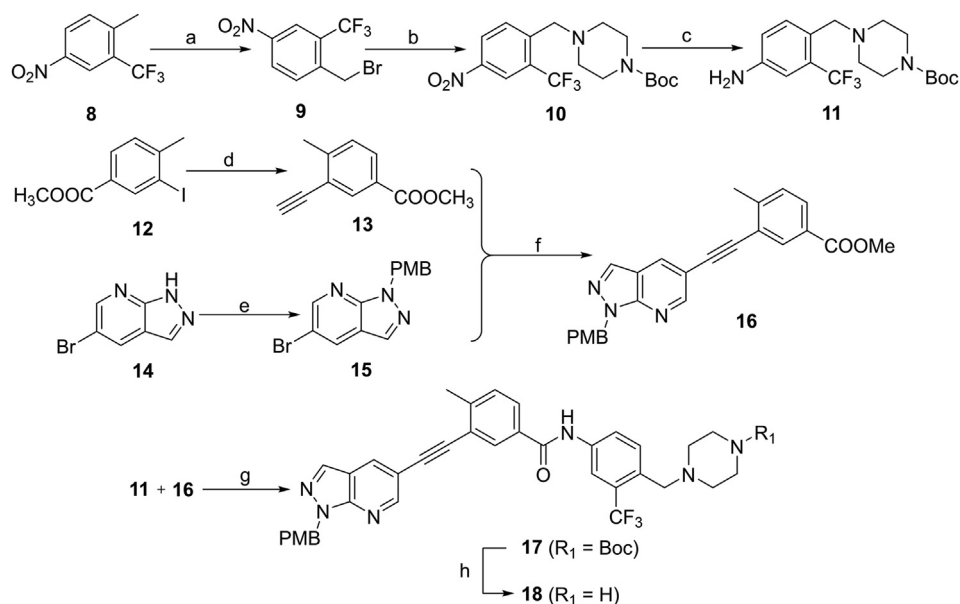


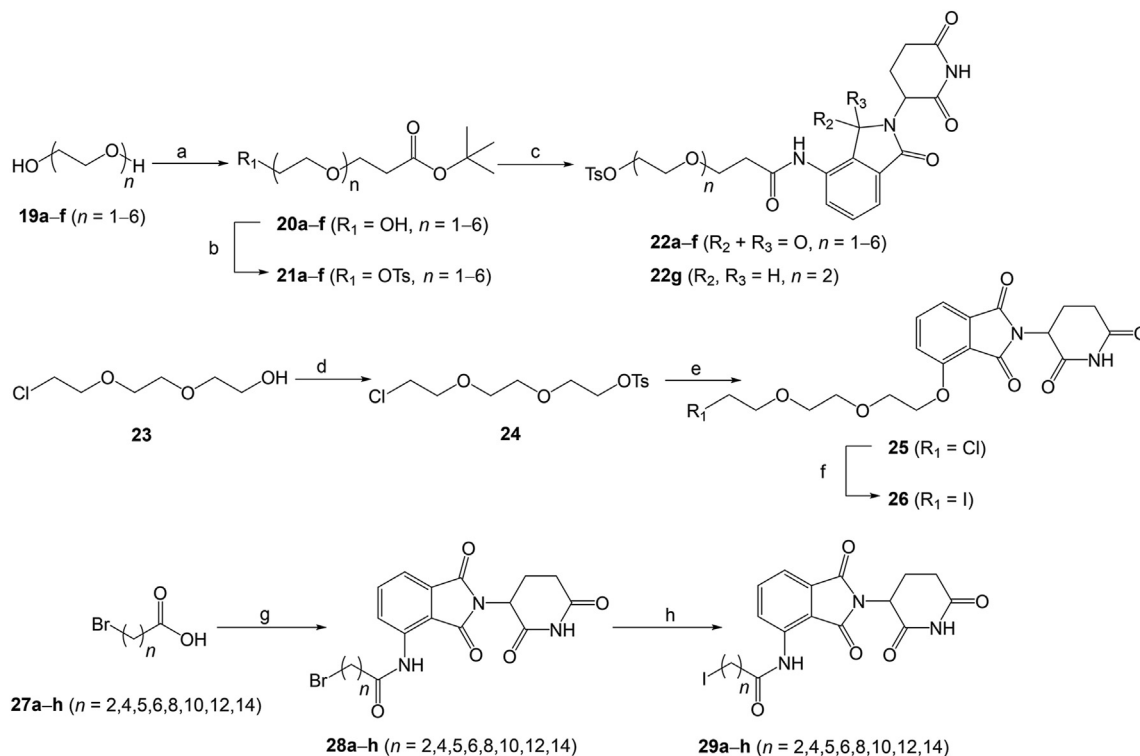
Figure 2 Design of Bcr-Abl^{T315I} PROTACs. (A) Chemical structures of Bcr-Abl^{T315I} inhibitor GZD824. (B) Proposed binding model of GZD824 with Abl protein. (C) General structure of the designed Bcr-Abl^{T315I} PROTACs.



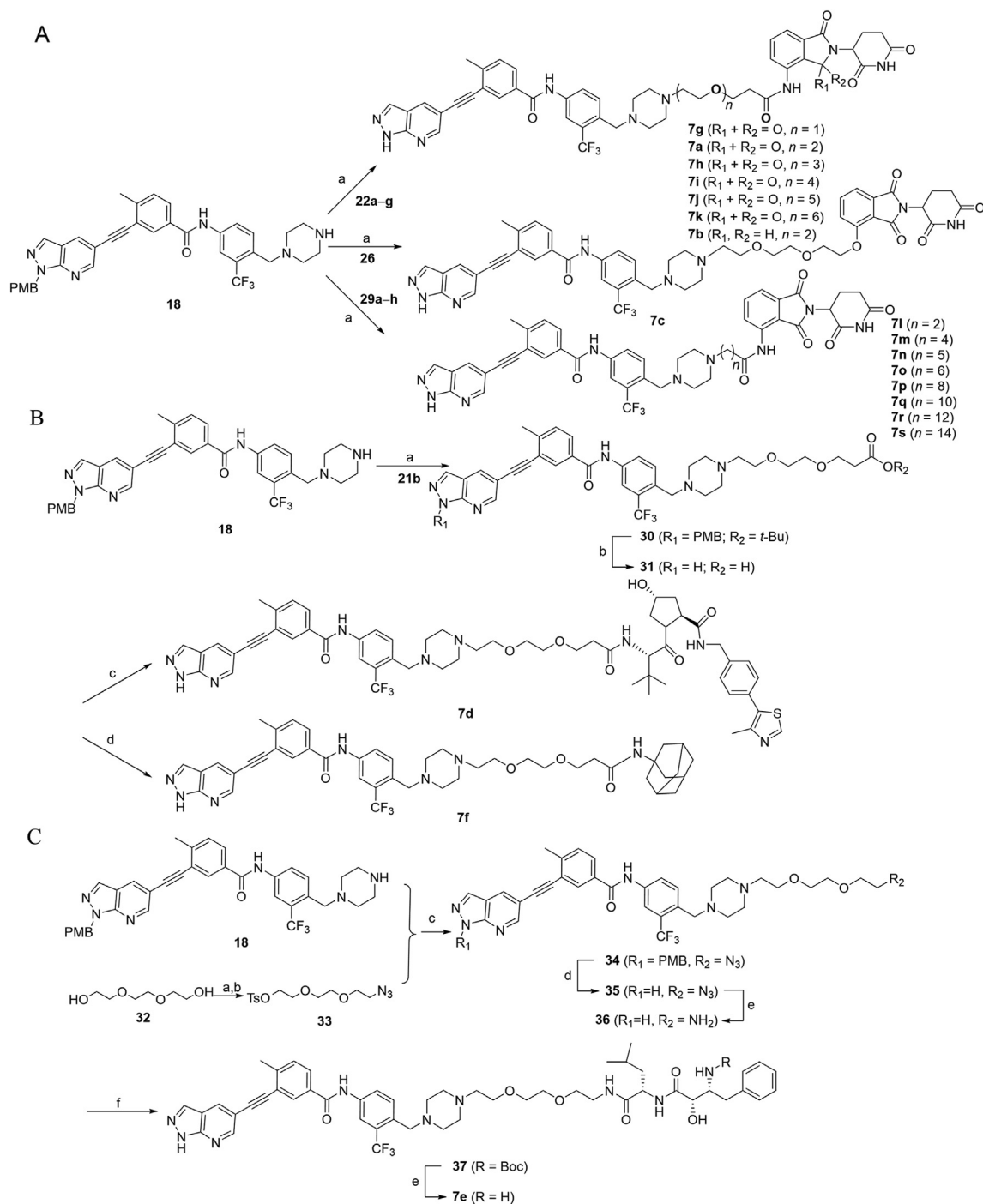
Scheme 1 Synthesis of the PMB protected POI ligand **18**. Reagents and conditions: (a) NBS, AIBN, DCE, 90 °C, overnight, 68%; (b) *N*-Boc-piperazine, Et₃N, DCM, rt, 5 h, 78%; (c) Fe, NH₄Cl, EtOH, H₂O, 80 °C, 10 h, 63.6%; (d) i) Pd(PPh₃)₂Cl₂, CuI, Et₃N, TMSA, MeCN, rt, overnight; ii) K₂CO₃, CH₃OH, rt, 1 h, 83%; (e) NaOH, PMBCl, DMF, rt, overnight, 32%; (f) Pd(PPh₃)₂Cl₂, CuI, Et₃N, DMF, 82 °C, 20 h, 56.4%; (g) *t*-BuOK, THF, -20 °C to rt, 3 h, 41.8%; (h) TFA, DCM, 1 h, 88%.

the degradation efficiency. These data suggested that the CRBN ligand pomalidomide might be utilized to design of Bcr-Abl^{T315I}

degrader. It was also noteworthy that the suppressed proliferation of compounds **7a–7f** against K562 and Ba/F3 Bcr-Abl^{WT} cell



Scheme 2 General synthesis of CRBN ligand conjugated linkers (**22a–22g**, **26** and **29a–29h**). Reagents and conditions: (a) Na, *tert*-butyl acrylate, THF, rt, 10 h, 21%–43%; (b) TsCl, Et₃N, DCM, 0 °C to rt, 10 h, 59%–82%; (c) TFA, DCM, rt, 2 h, then SOCl₂, reflux, 1 h, then pomalidomide or lenalidomide, THF, reflux, 4 h, 59%–80%; (d) TsCl, Et₃N, DCM, rt, 3 h, 79%; (e) KHCO₃, KI, thalidomide, DMF, 90 °C, 20 h, 49%; (f) NaI, acetone, reflux, 24 h; (g) SOCl₂, reflux, pomalidomide, THF, reflux, 4 h, 43%–77%; (h) NaI, acetone, reflux, 5 h.

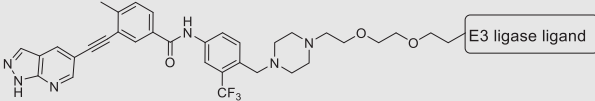


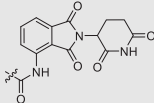
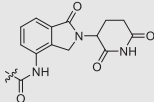
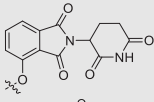
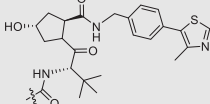
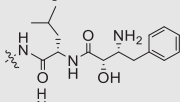
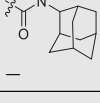
Scheme 3 General procedure for preparing PROTACs (**7a–7s**). (A) Synthesis of PROTACs **7a–7c** and **7g–7s**: (a) K_2CO_3 , MeCN, reflux, 10 h, TFA, 70°C , 5 h, 23%–75%. (B) Synthesis of PROTACs **7d** and **7f**: (a) K_2CO_3 , MeCN, reflux, 10 h, 51%; (b) TFA, 70°C , 5 h; (c) HATU, DIEA, DMF, rt, 10 h, 31%; (d) HATU, DIEA, DMF, rt, 10 h, 22%. (C) Synthesis of PROTAC **7e**: (a) TsCl, Et_3N , DCM, rt, 12 h, 79%; (b) NaN_3 , DMF, rt, 24 h, 40%. (c) K_2CO_3 , MeCN, reflux, 10 h, 61%; (d) TFA, 70°C , 5 h, 79%; (e) PPh_3 , THF, H_2O , rt, overnight, 51%; (f) ((2*S*,3*R*)-3-((*tert*-butoxycarbonyl)amino)-2-hydroxy-4-phenylbutanoyl)-*L*-leucine, HATU, DIEA, DMF, rt, 10 h; (e) TFA, DCM, 0°C to rt, 57%.

lines could be explained by the inhibitory activity of GZD824 against Bcr-Abl^{WT}.

To further examine the effect of linker length of compounds, using compound **7a** as a lead, we synthesized and evaluated compounds **7g–7k** by shortening or lengthening the length of **7a**'s linker with 1 and 3–6 PEG linker (Table 2). The results showed that **7h** containing 3

PEG exhibited about 2-fold improvement DR compared with **7a** (DR = 78.34%), while other compounds **7g** and **7i–7k** reduced the degradation activities with varying degrees (Table 2, Fig. S1). Unexpectedly, **7h** does not exhibit improvement antiproliferative activity against Ba/F3 Bcr-Abl^{T315I} cell lines compared with **7a**, which might be associated with the permeability of degrader. Nevertheless, the

Table 1 The degradation rate (DR) and cellular inhibition (IC₅₀) of designed PROTACs varying E3 ligase ligand.


Compd.	E3 ligase ligand	DR against Ba/F3 Bcr-Abl ^{T3151} (%)		Cellular inhibition IC ₅₀ (nmol/L)		
		100 nmol/L	300 nmol/L	K562	Ba/F3 Bcr-Abl ^{WT}	Ba/F3 Bcr-Abl ^{T3151}
7a		-15.35	39.01	7.9 ± 5.2	10.0 ± 2.1	83.2 ± 27.8
7b		-9.18	-4.21	4.0 ± 0.6	65.3 ± 30.2	286.9 ± 23.0
7c		-15.62	9.98	3.2 ± 0.1	22.4 ± 10.2	212.2 ± 101.1
7d		-18.26	-10.51	31.0 ± 0.1	336.6 ± 6.1	981.2 ± 24.9
7e		-14.92	11.17	58.6 ± 11.4	240.4 ± 75.4	2313.0 ± 424.0
7f		-5.26	11.72	>10,000	>10,000	>10,000
GZD824	—	2.59	20.62	1.6 ± 0.7	6.8 ± 5.3	31.0 ± 11.7

—Not applicable.

results demonstrated that shortening or excessive lengthening of the linker has adverse influence on the degradation potency of the PROTACs. The compound **7h** with linker “A” containing 3 PEG exhibits the most potent degradation efficacy.

Given that pure carbon chain was also utilized in the design for Bcr-Abl degraders^{23,24}, a series of new potential Bcr-Abl^{T3151} degraders **7l–7t** with 2–10 member length carbon chains were designed and synthesized. As shown in Table 2, among the derivatives, the generated compound **7o** with 6-member carbon chain exhibits the most potent degradation efficacy with DR of 69.89% and 94.23% at 100 and 300 nmol/L, respectively, and has an IC₅₀ value of 26.8 ± 9.7 nmol/L against Ba/F3 Bcr-Abl^{T3151} cells. When shortening or lengthening the length of carbon (*e.g.*, **7l–7n** and **7p–7t**) caused the reduction of degradation efficacy with varying degrees (Table 2, Fig. S1). Additionally, it was also noteworthy that although compounds **7m**, **7n** and **7p** exhibit equal antiproliferative activities to **7o** against Ba/F3 Bcr-Abl^{T3151} cells, they still exhibit weak degradation efficacy, while compound **7o** significantly decreased the level of Bcr-Abl^{T3151} protein with the degradation concentration (DC₅₀) value of 108.7 ± 16.3 nmol/L in Ba/F3 Bcr-Abl^{T3151} cells (Supporting Information Fig. S2).

2.4. Degradation mechanism examination

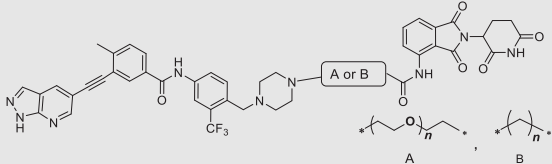
We next performed time-course studies to evaluate the time-dependent effect of Bcr-Abl^{T3151} degradation by compound **7o** in Ba/F3 cells expressed Bcr-Abl^{T3151}. Western blotting analysis suggested that **7o** caused the degradation of Bcr-Abl^{T3151} protein in a

time-dependent manner (Fig. 3A). **7o** reduced Bcr-Abl^{T3151} protein level substantially after 6 h treatment at 100 nmol/L, while appeared a “hook” effect during 8–10 h treatment. The maximum degradation was observed after 24 h treatment of **7o**. However, **7o** displayed a different trend for reducing Bcr-Abl^{WT} in K562 cells with substantially reduction after 36 h treatment at 100 nmol/L (Fig. 3B). The different manner degradation might be associated with the different states of E3 ligase in Ba/F3 Bcr-Abl^{T3151} and K562 cells.

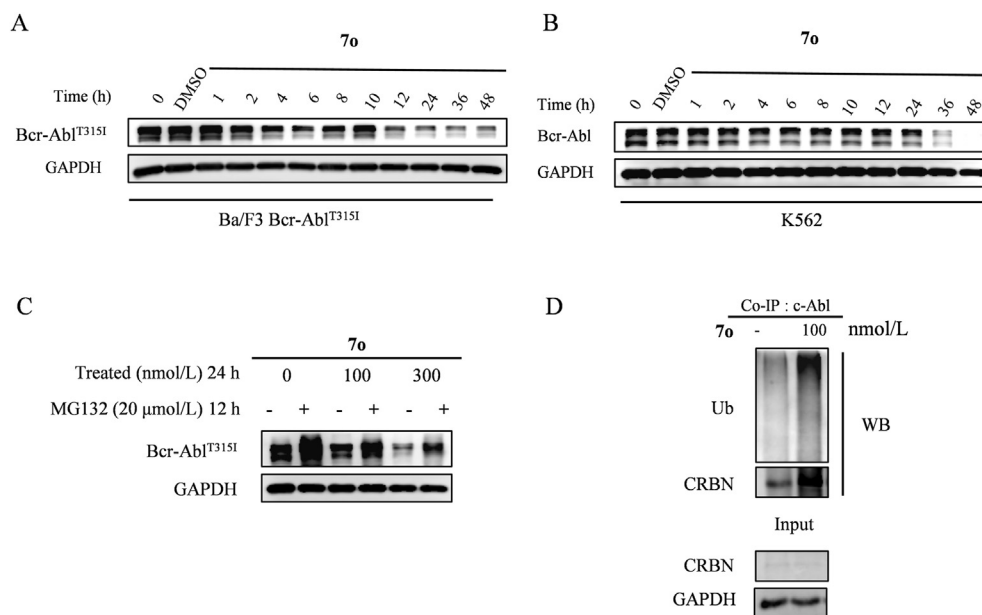
In order to elucidate the mechanism of **7o**-induced Bcr-Abl^{T3151} degradation, we further investigated the contribution of proteasome in protein degrading process. Ba/F3 Bcr-Abl^{T3151} cells were preincubated with 20 μmol/L proteasome inhibitor MG132, and then treated with **7o** for 24 h treatment at 100 and 300 nmol/L, respectively. The data suggested that MG132 can successfully rescue the Bcr-Abl^{T3151} degradation induced by **7o** (Fig. 3C). The co-immunoprecipitation (Co-IP) data demonstrated that the Bcr-Abl^{T3151} degradation induced by **7o** is mediated by CRBN E3 ubiquitin pathway (Fig. 3D).

2.5. Antitumor efficacy of compound **7o** in vivo

To evaluate the efficacy of compound **7o** *in vivo*, we first evaluated the *in vivo* pharmacokinetic properties of **7o** by a single intraperitoneal (i.p.) injection at a dose of 20 mg/kg. As show Fig. 4C, it was demonstrated that the high plasma concentrations maintained over 48 h and is expected to be sufficient to induce Bcr-Abl degradation *in vivo* study. The *in vivo* antitumor efficacy of compound **7o** was further examined in a Ba/F3 Bcr-Abl^{T3151} xenograft model. The

Table 2 The degradation rate (DR) and cellular inhibition (IC₅₀) of designed PROTACs varying the linkers.


Compd.	Linker	DR against Ba/F3 ^{T315I} (%)		Cellular inhibition IC ₅₀ (nmol/L)		
		100 nmol/L	300 nmol/L	K562	Ba/F3 Bcr-Abl ^{WT}	Ba/F3 Bcr-Abl ^{T315I}
7g	A, n = 1	-11.43	28.39	3.5 ± 0.5	20.7 ± 2.4	67.5 ± 3.2
7h	A, n = 3	16.86	78.34	13.7 ± 9.3	10.6 ± 2.6	83.4 ± 31.6
7i	A, n = 4	-22.44	-19.45	11.4 ± 7.3	19.9 ± 4.2	95.4 ± 37.4
7j	A, n = 5	-23.27	21.17	2.8 ± 0.4	14.3 ± 0.3	60.1 ± 0.3
7k	A, n = 6	19.38	25.53	10.5 ± 0.5	107.0 ± 24.9	305.6 ± 69.3
7l	B, n = 2	-30.35	37.19	2.1 ± 0.9	5.4 ± 0.8	65.8 ± 28.8
7m	B, n = 4	49.84	48.67	3.0 ± 1.2	4.3 ± 0.1	25.0 ± 10.4
7n	B, n = 5	21.64	30.39	2.1 ± 0.1	4.2 ± 0.3	33.4 ± 1.6
7o	B, n = 6	69.89	94.23	7.7 ± 1.8	4.2 ± 0.2	26.8 ± 9.7
7p	B, n = 8	3.61	63.47	14.0 ± 4.5	4.5 ± 0.0	21.8 ± 8.3
7q	B, n = 10	5.33	14.25	46.4 ± 21.2	36.1 ± 0.9	70.1 ± 34.3
7s	B, n = 12	-7.20	45.61	57.8 ± 19.5	61.0 ± 1.7	113.9 ± 29.9
7t	B, n = 14	13.75	28.73	190.3 ± 26.6	363.7 ± 2.4	399.4 ± 247.8
GZD824	—	2.59	20.62	1.6 ± 0.7	6.8 ± 5.3	31.0 ± 11.7

**Figure 3** Degradation mechanism study of PROTAC **7o** in Ba/F3 Bcr-Abl^{T315I}. Time-course studies of degradation by compound **7o** in Ba/F3 Bcr-Abl^{T315I} (A) and K562 (B). (C) PROTAC **7o** mediated Bcr-Abl^{T315I} degradation is rescued by proteasome inhibitor MG132. (D) PROTAC **7o** increased the ubiquitination level of ABL through CRBN E3 ligase.

animals were repeatedly administrated vehicle or compound **7o** once every two days *via* intraperitoneal injection (20 mg/kg, q2d) for 10 consecutive days. It was shown that compound **7o** obviously suppressed the growth of Ba/F3 Bcr-Abl^{T315I} xenograft tumor with a tumor growth inhibition (TGI) value of 90.8% at the dose of 20 mg/kg *in vivo* (Fig. 4A and C), and significantly induced the Bcr-Abl^{T315I} degradation (Fig. 4D) and apoptosis (Fig. 4E) in Ba/F3 Bcr-Abl^{T315I} xenograft tumor model. Additionally, there is no mortality or significant body weight loss (<5% relative to the vehicle matched controls)

observed during the treatment (Fig. 4B). All the results indicated that compound **7o** displayed significant *in vivo* anti-cancer activity and safety.

3. Conclusions

In this study, a new series of PROTAC degraders targeting Bcr-Abl^{T315I} which connect a phase II candidate GZD824 and E3 ligase ligands by ethyleneoxy and carbon chains linkers were

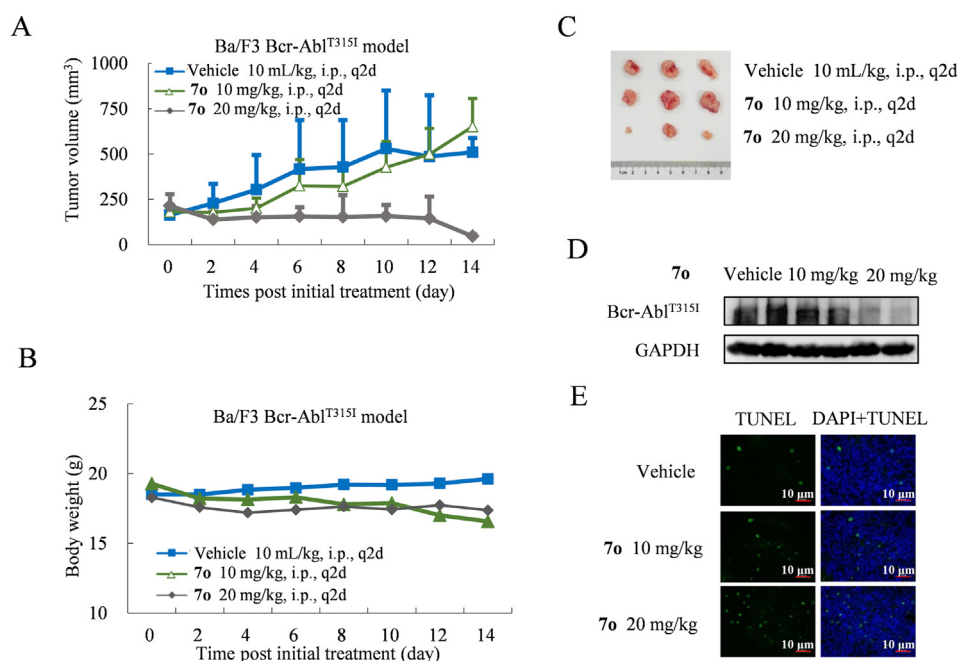


Figure 4 *In vivo* antitumor efficacy of Bcr-Abl^{T3151} degrader **7o** in the Ba/F3 Bcr-Abl^{T3151} xenograft models. (A) **7o** suppresses the growth of Ba/F3 Bcr-Abl^{T3151} *in vivo* at 10 and 20 mg/kg. (B) Effects of **7o** on body weight of mice in the Ba/F3 Bcr-Abl^{T3151} xenograft models. (C) Representative tumor images. (D) **7o** induced Bcr-Abl^{T3151} degradation at 20 mg/kg. (E) **7o** induced apoptosis *in vivo*.

designed, synthesized, and evaluated as anti-CML activity. Structure degradation relationships exploration led to the identification of the degrader **7o** with a 6-member carbon chain linkage with pomalidomide, which exhibits the most potent degradation efficacy with DR of 69.89% and 94.23% at 100 and 300 nmol/L, respectively. **7o** has an IC₅₀ value of 26.8 ± 9.7 nmol/L against Ba/F3 Bcr-Abl^{T3151} cells. Degradation mechanism study indicated that the degradation effect induced by **7o** was mediated by CRBN E3 ubiquitin pathway. Notably, **7o** displays substantial tumor regression against Ba/F3 Bcr-Abl^{T3151} xenograft model *in vivo*. To conclude, the study indicates that **7o** worth further investigation as a promising lead to overcome Bcr-Abl^{T3151} mutant induced clinical resistance.

4. Experimental

4.1. General method of chemistry

All chemicals were purchased from commercial vendors and used directly without further purification. All reactions requiring anhydrous conditions were carried out under argon atmosphere using oven-dried glassware. AR-grade solvents were used for all reactions. Reaction progress was monitored by TLC on pre-coated silica plates (Merck 60 F254 nm, 0.25 μm) and spots were visualized by UV, iodine or other suitable stains. Flash column chromatography was done using silica gel (Qingdao Ocean company). ¹H and ¹³C NMR spectra were recorded on a Bruker AV-400 spectrometer at 400 and 101 MHz, respectively. Coupling constants (*J*) are expressed in hertz (Hz). Chemical shifts (δ) of NMR are reported in parts per million (ppm) units relative to internal control (TMS). Mass spectra were obtained on Agilent LC-ESI-MS system. High resolution ESI-MS were recorded on an AB SCIEX X500r QTOF mass spectrometer. Purity of compounds was determined by reverse-phase high performance liquid chromatography (HPLC) analysis to be >95%. HPLC

instrument: Dionex Summit HPLC (column: Diamonsil C18, 5.0 μm, 4.6 mm × 250 mm (Dikma Technologies); detector: PDA-100 photodiode array; injector: ASI-100 autoinjector; pump: p-680A). A flow rate of 1.0 mL/min was used with mobile phase of MeOH in H₂O.

4.1.1. General procedure for the synthesis of **7a–c** and **7g–7s** (**7g** as example)

4.1.1.1. 3-((1*H*-Pyrazolo[3,4-*b*]pyridin-5-yl)ethynyl)-*N*-(4-((4-(2-(3-((2-(2,6-dioxopiperidin-3-yl)-1,3-dioxoisindolin-4-yl)amino)-3-oxopropoxy)ethyl)piperazin-1-yl)methyl)-3-(trifluoromethyl)phenyl)-4-methylbenzamide (**7g**). To a solution of **18** (610 mg, 0.96 mmol, 1 eq.) and **22a** (678 mg, 1.25 mmol, 1.3 eq.) in CH₃CN (30 mL), anhydrous K₂CO₃ (265 mg, 1.92 mmol, 2 eq.) was added and the mixture was stirred at reflux temperature for 10 h. Then, the solid is filtered off by suction and washed with DCM (2 × 25 mL), the filtrate is evaporated *in vacuo* and distilled at reduced pressure to get the crude product used without any further purification. Subsequently, the crude product (300 mg, 0.3 mmol, 1 eq.) was dissolved in TFA (10 mL), then it was stirred at 70 °C for 5 h. The mixture was then concentrated to an oil, which was partitioned between DCM and saturated with NaHCO₃. The aqueous layer was re-extracted with DCM and dried over Na₂SO₄, filtered and concentrated, the residue purified by flash column chromatography on silica gel (DCM:CH₃OH = 15:1) to afford the desired product as white solid (91 mg, 34% yield). ¹H NMR (400 MHz, DMSO-*d*₆) δ 13.96 (s, 1H), 11.16 (s, 1H), 10.55 (s, 1H), 9.88 (s, 1H), 8.75 (d, *J* = 2.0 Hz, 1H), 8.56–8.51 (m, 2H), 8.23 (s, 1H), 8.21 (t, *J* = 1.9 Hz, 2H), 8.07 (dd, *J* = 8.5, 2.2 Hz, 1H), 7.94 (dd, *J* = 8.0, 2.0 Hz, 1H), 7.80 (dd, *J* = 8.5, 7.3 Hz, 1H), 7.66 (d, *J* = 8.6 Hz, 1H), 7.59 (d, *J* = 7.3 Hz, 1H), 7.53 (d, *J* = 8.2 Hz, 1H), 5.15 (dd, *J* = 12.9, 5.4 Hz, 1H), 3.72 (t, *J* = 5.8 Hz, 2H), 3.57 (t, *J* = 5.6 Hz, 2H), 3.49 (s, 2H), 2.96–2.82 (m, 1H), 2.69 (t, *J* = 5.9 Hz, 2H), 2.65–2.54 (m, 7H), 2.47–2.34 (m, 4H),

2.34–2.21 (m, 4H), 2.09–1.99 (m, 1H). ^{13}C NMR (101 MHz, DMSO- d_6) δ 173.17, 170.97, 170.19, 168.14, 167.06, 165.16, 151.50, 151.03, 144.18, 138.61, 136.96, 136.58, 134.23, 133.49, 132.65, 132.45, 131.86, 131.62, 131.00, 130.42, 128.64, 127.95, 127.66, 126.36, 126.12, 123.95, 123.40, 122.64, 118.70, 117.01, 114.48, 112.25, 92.39, 88.76, 66.47, 57.89, 57.30, 53.52, 53.18, 49.36, 38.09, 31.39, 22.47, 20.93. HRMS (ESI) Calcd. for $\text{C}_{46}\text{H}_{42}\text{F}_3\text{N}_9\text{O}_7$ $[\text{M}+\text{H}]^+$, 890.3232; Found, 890.3213. HPLC purity = 97.36%, t_{R} 5.09 min.

4.1.1.2. 3-((1*H*-Pyrazolo[3,4-*b*]pyridin-5-yl)ethynyl)-*N*-(4-((2-(2-(3-((2-(2,6-dioxopiperidin-3-yl)-1,3-dioxoisindolin-4-yl)amino)-3-oxopropoxy)ethoxy)ethyl)piperazin-1-yl)methyl)-3-(trifluoromethyl)phenyl)-4-methylbenzamide (**7a**). White solid (42% yield). ^1H NMR (400 MHz, chloroform-*d*) δ 9.82 (s, 1H), 9.12 (s, 1H), 8.72 (d, J = 8.4 Hz, 1H), 8.54 (s, 1H), 8.08 (s, 1H), 8.04 (s, 1H), 7.96 (s, 1H), 7.91 (d, J = 10.0 Hz, 2H), 7.74 (d, J = 7.6 Hz, 1H), 7.59 (q, J = 8.6, 6.5 Hz, 2H), 7.43 (d, J = 7.2 Hz, 1H), 7.18 (d, J = 8.0 Hz, 1H), 4.94 (dd, J = 11.2, 5.8 Hz, 1H), 3.86–3.31 (m, 10H), 2.88–2.63 (m, 6H), 2.63–2.48 (m, 4H), 2.48–2.18 (m, 8H), 2.18–2.04 (m, 1H). ^{13}C NMR (101 MHz, chloroform-*d*) δ 172.36, 170.99, 169.28, 168.51, 166.88, 165.44, 151.31, 150.22, 144.09, 137.31, 137.15, 136.10, 133.95, 132.98, 132.01, 131.17, 130.5, 129.91, 128.97, 128.66, 125.58, 125.44, 123.46, 122.77, 118.42, 115.63, 114.57, 113.12, 91.28, 88.75, 70.41, 69.87, 68.29, 66.49, 57.64, 57.17, 53.31, 52.41, 49.25, 38.47, 31.59, 22.67, 20.77. HRMS (ESI) Calcd. for $\text{C}_{48}\text{H}_{46}\text{F}_3\text{N}_9\text{O}_8$ $[\text{M}+\text{H}]^+$, 934.3494; Found, 934.3468. HPLC purity = 99.53%, t_{R} 5.28 min.

4.1.1.3. 3-((1*H*-Pyrazolo[3,4-*b*]pyridin-5-yl)ethynyl)-*N*-(4-((2-(2-(3-((2-(2,6-dioxopiperidin-3-yl)-1-oxoisindolin-4-yl)amino)-3-oxopropoxy)ethoxy)ethyl)piperazin-1-yl)methyl)-3-(trifluoromethyl)phenyl)-4-methylbenzamide (**7b**). White solid (56% yield). ^1H NMR (400 MHz, methanol- d_4) δ 8.67 (d, J = 2.0 Hz, 1H), 8.40 (d, J = 2.0 Hz, 1H), 8.14 (s, 1H), 8.12 (d, J = 2.1 Hz, 2H), 7.92 (dd, J = 8.4, 2.2 Hz, 1H), 7.86–7.84 (m, 1H), 7.73 (d, J = 8.0 Hz, 1H), 7.69 (d, J = 8.6 Hz, 1H), 7.62 (d, J = 7.5 Hz, 1H), 7.48 (t, J = 7.7 Hz, 1H), 7.42 (d, J = 8.1 Hz, 1H), 5.17 (dd, J = 13.3, 5.2 Hz, 1H), 4.60–4.39 (m, 2H), 3.82 (t, J = 5.8 Hz, 2H), 3.69–3.50 (m, 8H), 2.95–2.83 (m, 1H), 2.81–2.71 (m, 1H), 2.67 (t, J = 5.9 Hz, 2H), 2.59 (s, 3H), 2.57–2.28 (m, 11H), 2.24–2.08 (m, 1H). ^{13}C NMR (101 MHz, methanol- d_4) δ 173.22, 171.00, 170.61, 169.63, 166.32, 151.32, 150.38, 144.10, 137.79, 134.87, 133.55, 133.16, 132.95, 132.53, 132.19, 131.12, 130.68, 129.62, 128.67, 127.46, 126.26, 123.62, 122.94, 120.06, 114.45, 113.0, 91.11, 88.10, 69.96, 69.86, 67.88, 66.63, 57.46, 57.14, 53.09, 52.19, 52.11, 36.54, 30.95, 22.83, 19.59. HRMS (ESI) Calcd. for $\text{C}_{48}\text{H}_{48}\text{N}_9\text{O}_7\text{F}_3$ $[\text{M}+\text{H}]^+$, 920.3702; Found, 920.3750. HPLC purity = 98.10%, t_{R} 6.05 min.

4.1.1.4. 3-((1*H*-Pyrazolo[3,4-*b*]pyridin-5-yl)ethynyl)-*N*-(4-((2-(2-(3-((2-(2,6-dioxopiperidin-3-yl)-1,3-dioxoisindolin-4-yl)oxy)ethoxy)ethoxy)ethyl)piperazin-1-yl)methyl)-3-(trifluoromethyl)phenyl)-4-methylbenzamide (**7c**). White solid (57% yield). ^1H NMR (400 MHz, methanol- d_4) δ 8.68 (d, J = 1.9 Hz, 1H), 8.41 (d, J = 2.0 Hz, 1H), 8.15 (s, 1H), 8.13 (d, J = 2.1 Hz, 1H), 8.12 (d, J = 2.4 Hz, 1H), 7.91 (dd, J = 8.6, 2.2 Hz, 1H), 7.87 (dd, J = 8.0, 2.0 Hz, 1H), 7.73–7.65 (m, 2H), 7.44 (d, J = 8.1 Hz, 1H), 7.41 (d, J = 3.1 Hz, 1H), 7.39 (d, J = 1.9 Hz, 1H), 5.08 (dd, J = 12.4, 5.5 Hz, 1H), 4.33 (t, J = 4.4 Hz, 2H), 3.94–3.87 (m,

2H), 3.79–3.74 (m, 2H), 3.72–3.67 (m, 2H), 3.66–3.62 (m, 2H), 3.60 (s, 2H), 2.92–2.62 (m, 9H), 2.60 (s, 3H), 2.51 (s, 4H), 2.15–2.05 (m, 1H). ^{13}C NMR (101 MHz, methanol- d_4) δ 173.16, 170.04, 167.06, 166.37, 165.90, 156.28, 151.32, 144.12, 137.92, 136.55, 133.63, 133.54, 132.97, 132.22, 132.17, 131.13, 130.70, 129.64, 129.44, 127.48, 123.64, 122.95, 119.29, 116.77, 115.34, 114.46, 113.03, 91.12, 88.09, 70.58, 69.97, 69.12, 68.97, 66.62, 57.25, 56.77, 52.73, 51.37, 49.04, 43.09, 30.77, 22.30, 19.59. HRMS (ESI) Calcd. for $\text{C}_{47}\text{H}_{45}\text{N}_8\text{O}_8\text{F}_3$ $[\text{M}+\text{H}]^+$, 907.3385; Found, 907.3387. HPLC purity = 100.00%, t_{R} 6.97 min.

4.1.1.5. 3-((1*H*-Pyrazolo[3,4-*b*]pyridin-5-yl)ethynyl)-*N*-(4-((2-(2-(3-((2-(2,6-dioxopiperidin-3-yl)-1,3-dioxoisindolin-4-yl)amino)-3-oxopropoxy)ethoxy)ethoxy)ethyl)piperazin-1-yl)methyl)-3-(trifluoromethyl)phenyl)-4-methylbenzamide (**7h**). White solid (36% yield). ^1H NMR (400 MHz, chloroform-*d*) δ 9.88 (s, 1H), 8.87 (s, 1H), 8.77 (d, J = 8.5 Hz, 1H), 8.60 (t, J = 1.9 Hz, 1H), 8.15 (d, J = 1.9 Hz, 1H), 8.08 (s, 1H), 8.00 (d, J = 1.8 Hz, 1H), 7.96–7.88 (m, 2H), 7.78 (dd, J = 7.9, 1.9 Hz, 1H), 7.70–7.55 (m, 2H), 7.48 (d, J = 7.3 Hz, 1H), 7.25 (d, J = 1.9 Hz, 1H), 4.95 (dd, J = 12.0, 5.4 Hz, 1H), 3.77 (t, J = 6.7 Hz, 2H), 3.73–3.68 (m, 2H), 3.68–3.59 (m, 4H), 3.59–3.46 (m, 6H), 2.90–2.82 (m, 1H), 2.82–2.72 (m, 2H), 2.71–2.65 (m, 2H), 2.63–2.34 (m, 13H), 2.18–2.10 (m, 1H). ^{13}C NMR (101 MHz, chloroform-*d*) δ 172.02, 171.13, 168.83, 168.52, 166.98, 165.27, 151.44, 150.30, 144.23, 137.43, 137.01, 136.11, 134.07, 133.16, 132.91, 132.05, 131.27, 131.23, 130.45, 130.04, 127.71, 125.67, 123.37, 122.92, 118.43, 114.62, 113.25, 88.78, 70.83, 70.40, 70.24, 68.01, 66.63, 57.69, 57.58, 53.28, 52.49, 49.36, 38.61, 31.60, 29.72, 22.78, 20.84. HRMS (ESI) Calcd. for $\text{C}_{50}\text{H}_{50}\text{F}_3\text{N}_9\text{O}_9$ $[\text{M}+\text{H}]^+$, 978.3756; Found, 978.3726. HPLC purity = 99.17%, t_{R} 5.38 min.

4.1.1.6. 1-(4-(4-(3-((1*H*-Pyrazolo[3,4-*b*]pyridin-5-yl)ethynyl)-4-methylbenzamide)-2-(trifluoromethyl)benzyl)piperazin-1-yl)-*N*-(2-(2,6-dioxopiperidin-3-yl)-1,3-dioxoisindolin-4-yl)-3,6,9,12-tetraoxapentadecan-15-amide (**7i**). White solid (40% yield). ^1H NMR (400 MHz, chloroform-*d*) δ 9.83 (s, 1H), 8.79 (d, J = 8.5 Hz, 1H), 8.68 (s, 1H), 8.52 (s, 1H), 8.22 (s, 1H), 8.11 (s, 1H), 8.03 (s, 1H), 7.91 (d, J = 9.8 Hz, 2H), 7.80 (d, J = 8.0 Hz, 1H), 7.74–7.59 (m, 2H), 7.50 (d, J = 7.3 Hz, 1H), 7.33 (d, J = 8.1 Hz, 1H), 4.99–4.88 (m, 1H), 3.80 (t, J = 5.7 Hz, 2H), 3.72–3.48 (m, 16H), 2.93–2.82 (m, 1H), 2.82–2.74 (m, 2H), 2.74–2.38 (m, 15H), 2.18–2.10 (m, 1H). ^{13}C NMR (101 MHz, chloroform-*d*) δ 171.64, 170.96, 168.60, 166.86, 165.11, 151.63, 150.38, 144.36, 137.48, 136.96, 136.18, 134.23, 133.16, 132.88, 132.07, 131.40, 131.24, 130.43, 130.14, 127.59, 125.63, 123.33, 123.10, 118.46, 115.67, 114.60, 113.39, 91.43, 88.77, 70.65, 70.53, 70.45, 70.25, 68.11, 66.57, 57.69, 57.45, 53.39, 52.30, 49.32, 38.58, 31.51, 22.76, 20.88. HRMS (ESI) Calcd. for $\text{C}_{52}\text{H}_{54}\text{F}_3\text{N}_9\text{O}_{10}$ $[\text{M}+\text{H}]^+$, 1022.4018; Found, 1022.3999. HPLC purity = 98.75%, t_{R} 5.42 min.

4.1.1.7. 1-(4-(4-(3-((1*H*-Pyrazolo[3,4-*b*]pyridin-5-yl)ethynyl)-4-methylbenzamide)-2-(trifluoromethyl)benzyl)piperazin-1-yl)-*N*-(2-(2,6-dioxopiperidin-3-yl)-1,3-dioxoisindolin-4-yl)-3,6,9,12,15-pentaoxaocetadecan-18-amide (**7j**). White solid (47% yield). ^1H NMR (400 MHz, chloroform-*d*) δ 9.82 (s, 1H), 8.78 (d, J = 8.6 Hz, 1H), 8.68 (d, J = 19.3 Hz, 2H), 8.20 (s, 1H), 8.09 (s, 1H), 8.04 (s, 1H), 7.92 (d, J = 7.5 Hz, 2H), 7.80 (d, J = 8.0 Hz, 1H), 7.73–7.59 (m, 2H), 7.49 (d, J = 7.4 Hz, 1H), 7.32 (t, J = 10.2 Hz, 1H), 5.04–4.82 (m, 1H), 3.80 (t,

$J = 5.8$ Hz, 2H), 3.75–3.44 (m, 20H), 2.93–2.81 (m, 1H), 2.81–2.74 (m, 2H), 2.73–2.28 (m, 15H), 2.18–2.10 (m, 1H). ^{13}C NMR (101 MHz, chloroform- d) δ 171.69, 170.94, 168.62, 168.56, 166.86, 165.18, 151.52, 150.35, 144.27, 137.46, 137.02, 136.15, 134.11, 133.20, 132.89, 132.12, 131.22, 130.48, 130.08, 127.65, 125.62, 123.35, 123.03, 118.44, 115.66, 114.61, 113.31, 91.40, 88.78, 70.63, 70.50, 70.45, 70.25, 68.37, 66.56, 57.72, 57.46, 53.39, 52.52, 49.30, 38.55, 31.51, 22.7, 20.87. HRMS (ESI) Calcd. for $\text{C}_{54}\text{H}_{58}\text{F}_3\text{N}_9\text{O}_{11}$ $[\text{M}+\text{H}]^+$, 1066.4281; Found, 1066.4259. HPLC purity = 98.17%, t_{R} 5.48 min.

4.1.1.8. 1-(4-(4-(3-((1H-Pyrazolo[3,4-*b*]pyridin-5-yl)ethynyl)-4-methylbenzamido)-2-(trifluoromethyl)benzyl)piperazin-1-yl)-*N*-(2-(2,6-dioxopiperidin-3-yl)-1,3-dioxoisindolin-4-yl)-3,6,9,12,15,18-hexaoxahenicosan-21-amide (**7k**). White solid (39% yield). ^1H NMR (400 MHz, chloroform- d) δ 9.82 (s, 1H), 8.84 (s, 1H), 8.78 (d, $J = 8.5$ Hz, 1H), 8.69 (d, $J = 1.9$ Hz, 1H), 8.24 (d, $J = 1.9$ Hz, 1H), 8.12 (s, 1H), 8.10 (d, $J = 2.0$ Hz, 1H), 8.03 (d, $J = 2.2$ Hz, 1H), 7.95 (dd, $J = 8.4, 2.2$ Hz, 1H), 7.85 (dd, $J = 7.9, 2.0$ Hz, 1H), 7.66 (dt, $J = 8.2, 3.7$ Hz, 2H), 7.51 (d, $J = 7.3$ Hz, 1H), 7.33 (d, $J = 8.2$ Hz, 1H), 5.03–4.93 (m, 1H), 3.81 (t, $J = 5.8$ Hz, 2H), 3.77 (t, $J = 4.9$ Hz, 2H), 3.70 (s, 4H), 3.67–3.46 (m, 18H), 2.99–2.74 (m, 9H), 2.75–2.60 (m, 6H), 2.55 (s, 3H), 2.25–2.08 (m, 1H). ^{13}C NMR (101 MHz, chloroform- d) δ 171.88, 170.90, 168.79, 168.54, 166.85, 165.34, 151.45, 150.28, 144.17, 137.41, 137.37, 136.14, 134.02, 132.93, 132.43, 131.98, 131.30, 131.17, 130.67, 129.97, 129.09, 128.79, 127.81, 125.58, 123.55, 122.90, 122.76, 118.44, 115.65, 114.58, 113.25, 91.36, 88.82, 70.56, 70.37, 70.32, 70.19, 67.37, 66.52, 57.57, 57.22, 53.25, 51.60, 49.30, 38.44, 31.49, 22.71, 20.83. HRMS (ESI) Calcd. for $\text{C}_{56}\text{H}_{68}\text{N}_9\text{O}_{12}\text{F}_3$ $[\text{M}+\text{H}]^+$, 1110.4669; Found, 1110.4618. HPLC purity = 100.00%, t_{R} 5.23 min.

4.1.1.9. 3-((1H-Pyrazolo[3,4-*b*]pyridin-5-yl)ethynyl)-*N*-(4-((4-(3-((2-(2,6-dioxopiperidin-3-yl)-1,3-dioxoisindolin-4-yl)amino)-3-oxopropyl)piperazin-1-yl)methyl)-3-(trifluoromethyl)phenyl)-4-methylbenzamide (**7l**). White solid (49% yield). ^1H NMR (400 MHz, chloroform- d) δ 10.61 (s, 1H), 8.82 (s, 1H), 8.75 (d, $J = 8.4$ Hz, 1H), 8.67 (d, $J = 1.9$ Hz, 1H), 8.21 (d, $J = 1.9$ Hz, 1H), 8.09 (s, 1H), 8.04 (d, $J = 2.0$ Hz, 1H), 7.96 (dd, $J = 8.5, 2.2$ Hz, 1H), 7.90 (d, $J = 2.2$ Hz, 1H), 7.79 (dd, $J = 7.9, 2.0$ Hz, 1H), 7.72 (d, $J = 8.6$ Hz, 1H), 7.67 (dd, $J = 8.5, 7.3$ Hz, 1H), 7.56–7.48 (m, 1H), 7.32 (d, $J = 8.1$ Hz, 1H), 4.96 (dd, $J = 12.1, 5.3$ Hz, 1H), 3.58 (s, 2H), 2.95–2.85 (m, 1H), 2.85–2.77 (m, 2H), 2.76–2.71 (m, 2H), 2.58 (d, $J = 28.8$ Hz, 13H), 2.19–2.13 (m, 1H). ^{13}C NMR (101 MHz, chloroform- d) δ 171.90, 171.48, 168.44, 167.88, 166.97, 165.32, 151.60, 150.41, 144.29, 137.25, 137.09, 135.94, 134.09, 133.17, 132.83, 132.16, 131.50, 131.42, 130.58, 130.04, 128.99, 128.69, 127.63, 126.69, 125.58, 123.54, 123.04, 118.61, 116.42, 114.55, 113.28, 91.45, 88.75, 57.74, 53.50, 52.95, 52.42, 49.29, 34.30, 31.47, 22.69, 20.91. HRMS (ESI) Calcd. for $\text{C}_{44}\text{H}_{38}\text{F}_3\text{N}_9\text{O}_6$ $[\text{M}+\text{H}]^+$, 846.2970; Found, 846.2968. HPLC purity = 99.23%, t_{R} 5.49 min.

4.1.1.10. 3-((1H-Pyrazolo[3,4-*b*]pyridin-5-yl)ethynyl)-*N*-(4-((4-(5-((2-(2,6-dioxopiperidin-3-yl)-1,3-dioxoisindolin-4-yl)amino)-5-oxopentyl)piperazin-1-yl)methyl)-3-(trifluoromethyl)phenyl)-4-methylbenzamide (**7m**). White solid (38% yield). ^1H NMR (400 MHz, DMSO- d_6) δ 13.98 (s, 1H), 11.19 (s, 1H), 10.59 (s, 1H), 9.73 (s, 1H), 8.74 (d, $J = 2.0$ Hz, 1H), 8.52 (d, $J = 2.0$ Hz, 1H), 8.45 (d, $J = 8.4$ Hz, 1H), 8.27–8.15 (m, 3H), 8.10 (d,

$J = 8.5$ Hz, 1H), 7.93 (d, $J = 8.0$ Hz, 1H), 7.82 (t, $J = 7.9$ Hz, 1H), 7.70 (d, $J = 8.5$ Hz, 1H), 7.61 (d, $J = 7.3$ Hz, 1H), 7.52 (d, $J = 8.2$ Hz, 1H), 5.15 (dd, $J = 12.7, 5.4$ Hz, 1H), 3.59 (s, 2H), 2.96–2.82 (m, 1H), 2.74–2.25 (m, 17H), 2.11–2.00 (m, 1H), 1.70–1.50 (m, 4H). ^{13}C NMR (101 MHz, DMSO- d_6) δ 173.22, 172.25, 170.24, 168.14, 167.11, 165.16, 151.48, 151.03, 144.18, 138.80, 136.95, 136.54, 134.17, 133.45, 132.58, 132.02, 131.89, 131.73, 131.01, 130.39, 128.61, 128.04, 127.75, 126.78, 126.13, 123.95, 122.65, 118.79, 117.46, 114.47, 112.25, 92.38, 88.75, 57.57, 52.56, 49.38, 46.05, 36.51, 31.41, 22.79, 22.47, 20.91. HRMS (ESI) Calcd. for $\text{C}_{46}\text{H}_{42}\text{F}_3\text{N}_9\text{O}_6$ $[\text{M}+\text{H}]^+$, 874.3283; Found, 874.3280. HPLC purity = 97.74%, t_{R} 5.60 min.

4.1.1.11. 3-((1H-Pyrazolo[3,4-*b*]pyridin-5-yl)ethynyl)-*N*-(4-((4-(6-((2-(2,6-dioxopiperidin-3-yl)-1,3-dioxoisindolin-4-yl)amino)-6-oxohexyl)piperazin-1-yl)methyl)-3-(trifluoromethyl)phenyl)-4-methylbenzamide (**7n**). White solid (29% yield). ^1H NMR (400 MHz, DMSO- d_6) δ 13.95 (s, 1H), 11.16 (s, 1H), 10.53 (s, 1H), 9.68 (s, 1H), 8.73 (d, $J = 2.0$ Hz, 1H), 8.51 (d, $J = 2.0$ Hz, 1H), 8.47 (d, $J = 8.4$ Hz, 1H), 8.22 (s, 1H), 8.19 (dd, $J = 7.4, 2.1$ Hz, 2H), 8.06 (dd, $J = 8.4, 2.2$ Hz, 1H), 7.92 (dd, $J = 8.0, 2.0$ Hz, 1H), 7.85–7.78 (m, 1H), 7.69 (d, $J = 8.5$ Hz, 1H), 7.59 (d, $J = 7.3$ Hz, 1H), 7.51 (d, $J = 8.2$ Hz, 1H), 5.14 (dd, $J = 12.7, 5.5$ Hz, 1H), 3.53 (s, 2H), 2.95–2.80 (m, 1H), 2.65–2.52 (m, 6H), 2.48–2.29 (m, 9H), 2.26 (t, $J = 7.2$ Hz, 2H), 2.10–1.98 (m, 1H), 1.62 (p, $J = 7.5$ Hz, 2H), 1.44 (p, $J = 7.3$ Hz, 2H), 1.36–1.25 (m, 2H). ^{13}C NMR (101 MHz, DMSO- d_6) δ 173.21, 172.47, 170.24, 168.17, 167.11, 165.15, 151.50, 151.03, 144.18, 138.61, 137.02, 136.56, 134.20, 133.48, 132.63, 132.53, 131.88, 131.65, 130.99, 130.42, 128.62, 127.97, 127.68, 126.68, 126.15, 123.95, 123.43, 122.6, 118.73, 117.35, 114.48, 112.25, 92.38, 88.76, 58.10, 57.93, 53.25, 49.36, 36.96, 31.40, 26.86, 26.43, 25.19, 22.45, 20.92. HRMS (ESI) Calcd. for $\text{C}_{47}\text{H}_{44}\text{N}_9\text{O}_6\text{F}_3$ $[\text{M}+\text{H}]^+$, 888.3439; Found, 888.3469. HPLC purity = 100.00%, t_{R} 9.70 min.

4.1.1.12. 3-((1H-Pyrazolo[3,4-*b*]pyridin-5-yl)ethynyl)-*N*-(4-((4-(7-((2-(2,6-dioxopiperidin-3-yl)-1,3-dioxoisindolin-4-yl)amino)-7-oxoheptyl)piperazin-1-yl)methyl)-3-(trifluoromethyl)phenyl)-4-methylbenzamide (**7o**). White solid (75% yield). ^1H NMR (400 MHz, DMSO- d_6) δ 13.96 (s, 1H), 11.17 (s, 1H), 10.60 (s, 1H), 9.68 (s, 1H), 8.73 (d, $J = 2.0$ Hz, 1H), 8.51 (d, $J = 2.0$ Hz, 1H), 8.46 (d, $J = 8.4$ Hz, 1H), 8.24–8.20 (m, 2H), 8.19 (d, $J = 2.0$ Hz, 1H), 8.10 (dd, $J = 8.5, 2.2$ Hz, 1H), 7.93 (dd, $J = 8.0, 2.0$ Hz, 1H), 7.81 (dd, $J = 8.5, 7.3$ Hz, 1H), 7.70 (d, $J = 8.6$ Hz, 1H), 7.60 (d, $J = 7.3$ Hz, 1H), 7.51 (d, $J = 8.2$ Hz, 1H), 5.15 (dd, $J = 12.7, 5.4$ Hz, 1H), 3.62 (s, 2H), 2.96–2.68 (m, 6H), 2.67–2.51 (m, 8H), 2.48–2.32 (m, 4H), 2.11–2.02 (m, 1H), 1.67–1.50 (m, 4H), 1.40–1.24 (m, 4H). ^{13}C NMR (101 MHz, DMSO- d_6) δ 173.27, 172.47, 170.29, 168.15, 167.12, 165.12, 151.49, 150.99, 144.18, 138.62, 136.98, 136.55, 134.19, 133.48, 132.57, 132.42, 131.86, 131.62, 130.98, 130.41, 128.63, 127.94, 127.65, 126.68, 126.13, 123.92, 123.41, 122.61, 118.74, 117.32, 114.47, 112.23, 92.36, 88.74, 58.12, 57.85, 53.15, 49.34, 36.93, 31.39, 28.90, 27.09, 25.21, 22.45, 20.92. HRMS (ESI) Calcd. for $\text{C}_{48}\text{H}_{46}\text{F}_3\text{N}_9\text{O}_6$ $[\text{M}+\text{H}]^+$, 902.3596; Found, 902.3582. HPLC purity = 99.87%, t_{R} 7.29 min.

4.1.1.13. 3-((1H-Pyrazolo[3,4-*b*]pyridin-5-yl)ethynyl)-*N*-(4-((4-(9-((2-(2,6-dioxopiperidin-3-yl)-1,3-dioxoisindolin-4-yl)amino)-9-oxononyl)piperazin-1-yl)methyl)-3-(trifluoromethyl)phenyl)-4-methylbenzamide (**7p**). White solid (23% yield). ^1H NMR

(400 MHz, DMSO- d_6) δ 13.96 (s, 1H), 11.18 (s, 1H), 10.55 (s, 1H), 9.68 (s, 1H), 8.74 (d, J = 2.0 Hz, 1H), 8.52 (d, J = 2.0 Hz, 1H), 8.48 (d, J = 8.4 Hz, 1H), 8.22 (d, J = 4.2 Hz, 2H), 8.20 (d, J = 2.0 Hz, 1H), 8.08 (dd, J = 8.4, 2.2 Hz, 1H), 7.93 (dd, J = 7.9, 2.0 Hz, 1H), 7.82 (t, J = 7.9 Hz, 1H), 7.70 (d, J = 8.6 Hz, 1H), 7.60 (d, J = 7.2 Hz, 1H), 7.52 (d, J = 8.3 Hz, 1H), 5.16 (dd, J = 12.7, 5.4 Hz, 1H), 3.56 (s, 2H), 2.90–2.81 (m, 1H), 2.66–2.51 (m, 6H), 2.47–2.21 (m, 11H), 2.11–2.00 (m, 1H), 1.62 (p, J = 7.3 Hz, 2H), 1.34–1.15 (m, 10H). ^{13}C NMR (101 MHz, DMSO- d_6) δ 173.21, 172.46, 170.24, 168.18, 167.11, 165.13, 151.49, 151.03, 144.17, 138.66, 137.03, 136.55, 134.18, 133.46, 132.61, 132.43, 131.88, 131.65, 130.99, 130.40, 128.62, 127.99, 127.69, 126.63, 126.15, 123.93, 123.43, 122.64, 118.71, 117.31, 114.48, 112.25, 92.38, 88.76, 58.16, 57.86, 53.13, 49.37, 37.00, 31.41, 29.26, 29.17, 28.94, 27.29, 26.80, 25.22, 22.47, 20.92. HRMS (ESI) Calcd. for $\text{C}_{50}\text{H}_{50}\text{F}_3\text{N}_9\text{O}_6$ $[\text{M}+\text{H}]^+$, 930.3909; Found, 930.3898. HPLC purity = 99.83%, t_{R} 8.97 min.

4.1.1.14. 3-((1*H*-Pyrazolo[3,4-*b*]pyridin-5-yl)ethynyl)-*N*-(4-((11-((2-(2,6-dioxopiperidin-3-yl)-1,3-dioxoisindolin-4-yl)amino)-11-oxoundecyl)piperazin-1-yl)methyl)-3-(trifluoromethyl)phenyl)-4-methylbenzamide (**7q**). White solid (50% yield). ^1H NMR (400 MHz, DMSO- d_6) δ 13.97 (s, 1H), 11.20 (s, 1H), 10.55 (s, 1H), 9.67 (s, 1H), 8.72 (s, 1H), 8.48 (dd, J = 21.8, 8.1 Hz, 2H), 8.20 (t, J = 8.5 Hz, 3H), 8.06 (d, J = 8.4 Hz, 1H), 7.91 (d, J = 7.9 Hz, 1H), 7.81–7.73 (m, 1H), 7.69 (d, J = 8.9 Hz, 1H), 7.58 (t, J = 6.4 Hz, 1H), 7.52–7.47 (m, 1H), 5.14 (dd, J = 12.6, 5.5 Hz, 1H), 3.56 (s, 2H), 3.00–2.81 (m, 1H), 2.66–2.51 (m, 6H), 2.45–2.16 (m, 11H), 2.12–1.98 (m, 1H), 1.63–1.51 (m, 2H), 1.45–1.08 (m, 14H). ^{13}C NMR (101 MHz, DMSO- d_6) δ 173.27, 172.48, 170.28, 168.18, 167.11, 165.12, 151.49, 150.98, 144.18, 138.60, 136.99, 136.54, 134.19, 133.48, 132.55, 132.45, 131.84, 131.60, 130.97, 130.40, 128.61, 127.94, 127.64, 126.62, 126.13, 123.89, 123.40, 122.61, 118.71, 117.62, 114.46, 112.24, 92.35, 88.74, 58.26, 57.88, 53.18, 49.33, 36.97, 31.39, 29.44, 29.37, 29.21, 28.98, 27.40, 26.66, 25.22, 22.45, 20.91. HRMS (ESI) Calcd. for $\text{C}_{52}\text{H}_{54}\text{F}_3\text{N}_9\text{O}_6$ $[\text{M}+\text{H}]^+$, 958.4222; Found, 958.4210. HPLC purity = 99.00%, t_{R} 12.25 min.

4.1.1.15. 3-((1*H*-Pyrazolo[3,4-*b*]pyridin-5-yl)ethynyl)-*N*-(4-((13-((2-(2,6-dioxopiperidin-3-yl)-1,3-dioxoisindolin-4-yl)amino)-13-oxotridecyl)piperazin-1-yl)methyl)-3-(trifluoromethyl)phenyl)-4-methylbenzamide (**7r**). White solid (52% yield). ^1H NMR (400 MHz, DMSO- d_6) δ 13.95 (s, 1H), 11.16 (s, 1H), 10.54 (s, 1H), 9.67 (s, 1H), 8.73 (d, J = 1.9 Hz, 1H), 8.52 (d, J = 1.9 Hz, 1H), 8.47 (d, J = 8.4 Hz, 1H), 8.21 (d, J = 3.9 Hz, 2H), 8.19 (d, J = 1.8 Hz, 1H), 8.07 (dd, J = 8.5, 2.1 Hz, 1H), 7.92 (dd, J = 8.0, 1.9 Hz, 1H), 7.81 (t, J = 7.9 Hz, 1H), 7.69 (d, J = 8.5 Hz, 1H), 7.59 (d, J = 7.3 Hz, 1H), 7.52 (d, J = 8.1 Hz, 1H), 5.14 (dd, J = 12.7, 5.4 Hz, 1H), 3.56 (s, 2H), 2.96–2.80 (m, 1H), 2.66–2.53 (m, 6H), 2.47–2.19 (m, 11H), 2.11–1.99 (m, 1H), 1.60 (p, J = 7.2 Hz, 2H), 1.31–1.17 (m, 18H). ^{13}C NMR (101 MHz, DMSO- d_6) δ 173.20, 172.46, 170.23, 168.17, 167.12, 165.13, 151.49, 151.03, 144.17, 138.66, 137.03, 136.55, 134.19, 133.47, 132.61, 132.44, 131.88, 131.65, 131.00, 130.41, 128.62, 126.65, 123.94, 122.64, 118.71, 117.32, 114.48, 112.25, 92.38, 88.76, 58.14, 57.88, 53.14, 49.37, 36.99, 31.41, 29.39, 29.20,

28.97, 27.33, 26.52, 25.23, 22.46, 20.92. HRMS (ESI) Calcd. for $\text{C}_{54}\text{H}_{58}\text{F}_3\text{N}_9\text{O}_6$ $[\text{M}+\text{H}]^+$, 986.4535; Found, 986.4522. HPLC purity = 98.84%, t_{R} 7.40 min.

4.1.1.16. 3-((1*H*-Pyrazolo[3,4-*b*]pyridin-5-yl)ethynyl)-*N*-(4-((15-((2-(2,6-dioxopiperidin-3-yl)-1,3-dioxoisindolin-4-yl)amino)-15-oxopentadecyl)piperazin-1-yl)methyl)-3-(trifluoromethyl)phenyl)-4-methylbenzamide (**7s**). White solid (43% yield). ^1H NMR (400 MHz, chloroform-*d*) δ 9.40 (s, 1H), 8.81 (d, J = 8.4 Hz, 1H), 8.68 (d, J = 1.9 Hz, 1H), 8.40 (s, 1H), 8.22 (d, J = 1.8 Hz, 1H), 8.12 (s, 1H), 8.01 (d, J = 1.9 Hz, 1H), 7.91 (d, J = 9.5 Hz, 2H), 7.79 (dd, J = 8.1, 1.9 Hz, 1H), 7.74 (d, J = 8.3 Hz, 1H), 7.68 (t, J = 7.9 Hz, 1H), 7.51 (d, J = 7.3 Hz, 1H), 7.33 (d, J = 8.2 Hz, 1H), 4.96 (dd, J = 12.2, 5.4 Hz, 1H), 3.61 (s, 2H), 2.95–2.85 (m, 1H), 2.84–2.69 (m, 2H), 2.60–2.38 (m, 11H), 2.34 (t, J = 7.9 Hz, 2H), 2.20–2.12 (m, 1H), 1.72 (p, J = 7.5 Hz, 2H), 1.53–1.42 (m, 2H), 1.37–1.14 (m, 22H). ^{13}C NMR (101 MHz, chloroform-*d*) δ 172.54, 171.37, 169.19, 168.44, 166.77, 165.08, 151.59, 150.39, 144.39, 137.87, 136.70, 136.42, 134.21, 133.69, 132.92, 132.11, 131.38, 131.05, 130.34, 130.17, 127.50, 125.27, 123.31, 123.15, 118.40, 115.23, 114.64, 113.38, 91.43, 88.73, 58.70, 57.80, 53.2, 53.03, 49.32, 38.02, 31.48, 29.71, 29.50, 29.45, 29.37, 29.22, 29.11, 27.58, 26.59, 25.24, 22.71, 20.89. HRMS (ESI) Calcd. for $\text{C}_{56}\text{H}_{62}\text{F}_3\text{N}_9\text{O}_6$ $[\text{M}+\text{H}]^+$, 1014.4848; Found, 1014.4826. HPLC purity = 99.05%, t_{R} 9.62 min.

4.1.2. Procedure for the synthesis of **7d** and **7e**

4.1.2.1. 3-((1*H*-Pyrazolo[3,4-*b*]pyridin-5-yl)ethynyl)-*N*-(4-((2-(2-(3-(((2*S*)-1-((2*R*,4*S*)-4-hydroxy-2-((4-(4-methylthiazol-5-yl)benzyl)carbamoyl)cyclopentyl)-3,3-dimethyl-1-oxobutan-2-yl)amino)-3-oxopropoxy)ethoxy)ethyl)piperazin-1-yl)methyl)-3-(trifluoromethyl)phenyl)-4-methylbenzamide (**7d**). To a solution of **31** (50 mg, 0.073 mmol, 1 eq.) in DMF (5 mL) was added HATU (55 mg, 0.15 mmol, 2 eq.) and the resulting solution stirred for 10 min at rt after which VHL ligand (66 mg, 0.15 mmol, 2.1 eq.) and DIEA (66 mg, 0.52 mmol, 7 eq.) were added respectively. The resulting mixture was stirred at room temperature for 10 h. The product was extracted twice with EtOAc then the residue purified by flash column chromatography on silica gel (DCM:CH₃OH = 10:1) to afford the desired product as white solid (25 mg, 31% yield). ^1H NMR (400 MHz, DMSO- d_6) δ 10.57 (s, 1H), 8.97 (s, 1H), 8.73 (d, J = 2.0 Hz, 1H), 8.22 (s, 1H), 8.21 (s, 1H), 8.19 (d, J = 1.9 Hz, 1H), 8.07 (dd, J = 8.4, 2.2 Hz, 1H), 7.95–7.93 (m, 1H), 7.92–7.90 (m, 1H), 7.71 (d, J = 8.5 Hz, 1H), 7.53 (d, J = 8.2 Hz, 1H), 7.43–7.35 (m, 4H), 5.15 (s, 1H), 4.55 (d, J = 9.4 Hz, 1H), 4.48–4.37 (m, 2H), 4.34 (s, 1H), 4.21 (dd, J = 15.9, 5.5 Hz, 1H), 3.70–3.52 (m, 6H), 3.51–3.42 (m, 6H), 2.59 (s, 3H), 2.55 (d, J = 7.6 Hz, 1H), 2.47–2.29 (m, 13H), 2.07–1.96 (m, 1H), 1.93–1.85 (m, 1H), 1.23 (s, 2H), 0.93 (s, 9H). ^{13}C NMR (101 MHz, DMSO- d_6) δ 172.41, 170.45, 169.99, 165.19, 151.90, 151.51, 148.16, 144.20, 139.94, 138.65, 133.51, 132.62, 131.69, 131.62, 131.00, 130.44, 130.09, 129.09, 127.87, 123.96, 122.64, 114.49, 112.25, 92.38, 88.76, 70.07, 69.90, 69.34, 67.38, 59.18, 56.84, 56.77, 53.46, 42.11, 38.40, 36.12, 35.83, 26.78, 20.92, 16.39. HRMS (ESI) Calcd. for $\text{C}_{57}\text{H}_{65}\text{N}_{10}\text{O}_7\text{F}_3\text{S}$

$[M+H]^+$, 1091.4883; Found, 1091.4777. HPLC purity = 99.39%, t_R 11.05 min.

4.1.2.2. 3-((1H-Pyrazolo[3,4-b]pyridin-5-yl)ethynyl)-N-(4-((2-(2-(3-(adamantan-1-ylamino)-3-oxopropoxy)ethoxy)ethyl)piperazin-1-yl)methyl)-3-(trifluoromethyl)phenyl)-4-methylbenzamide (7f). To a solution of **31** (50 mg, 0.073 mmol, 1 eq.) in DMF (5 mL) was added HATU (55 mg, 0.15 mmol, 2 eq.) and the resulting solution stirred for 10 min at room temperature after which adamantan-1-amine (23 mg, 0.15 mmol, 2.1 eq.) and DIEA (66 mg, 0.52 mmol, 7 eq.) were added respectively. The resulting mixture was stirred at room temperature for 10 h. The product was extracted twice with EtOAc then the residue purified by flash column chromatography on silica gel (DCM:CH₃OH = 20:1) to afford the desired product as white solid (13 mg, 22% yield). ¹H NMR (400 MHz, chloroform-*d*) δ 8.75 (d, *J* = 2.1 Hz, 1H), 8.60 (s, 1H), 8.17 (d, *J* = 2.1 Hz, 1H), 8.06 (s, 1H), 8.05 (d, *J* = 2.0 Hz, 1H), 7.95 (d, *J* = 2.2 Hz, 1H), 7.92 (d, *J* = 2.2 Hz, 1H), 7.80 (dd, *J* = 8.0, 2.0 Hz, 1H), 7.74 (d, *J* = 8.4 Hz, 1H), 7.34 (d, *J* = 8.0 Hz, 1H), 6.00 (s, 1H), 3.66 (t, *J* = 5.8 Hz, 2H), 3.62–3.59 (m, 3H), 3.59–3.56 (m, 5H), 2.61–2.55 (m, 6H), 2.55–2.41 (m, 6H), 2.34 (t, *J* = 5.8 Hz, 2H), 2.09–2.00 (m, 4H), 1.98–1.94 (m, 6H), 1.66–1.62 (m, 6H). ¹³C NMR (101 MHz, chloroform-*d*) δ 170.65, 165.34, 156.57, 153.19, 144.22, 137.03, 133.37, 132.55, 132.25, 131.27, 130.49, 130.01, 129.24, 128.94, 127.43, 125.48, 123.46, 123.28, 119.68, 113.22, 112.76, 92.43, 88.65, 70.34, 70.18, 68.73, 67.62, 61.44, 57.81, 53.71, 52.93, 51.68, 41.57, 38.15, 36.38, 29.92, 29.41, 20.91. HRMS (ESI) Calcd. for C₄₉H₆₀N₇O₄F₃ $[M+H]^+$, 812.4106; Found 812.4112. HPLC purity = 99.56%, t_R 12.00 min.

4.1.2.3. 3-((1H-Pyrazolo[3,4-b]pyridin-5-yl)ethynyl)-N-(4-((11S,14S,15R)-15-amino-14-hydroxy-11-isobutyl-10,13-dioxo-16-phenyl-3,6-dioxo-9,12-diazahexadecyl)piperazin-1-yl)methyl)-3-(trifluoromethyl)phenyl)-4-methylbenzamide (7e). To a solution of **38** (25 mg, 0.024 mmol) in DCM (6 mL), cooled to 0 °C was added TFA (2 mL). After 1 h the consumption of the starting material (monitored by TLC), the mixture was evaporated and then saturated aqueous NaHCO₃ was added. The aqueous layer was extracted twice with DCM (30 mL), and the organic layer washed with brine and dried over anhydrous Na₂SO₄. The solvent was removed under vacuum, the residue purified by flash column chromatography on silica gel (DCM:CH₃OH = 15:1) to afford the desired product as white solid (13 mg, 57% yield). ¹H NMR (400 MHz, DMSO-*d*₆) δ 10.56 (s, 1H), 8.74 (d, *J* = 2.1 Hz, 1H), 8.53 (d, *J* = 2.0 Hz, 1H), 8.26 (t, *J* = 5.6 Hz, 1H), 8.23 (s, 1H), 8.22 (d, *J* = 2.2 Hz, 1H), 8.20 (d, *J* = 1.9 Hz, 1H), 8.07 (dd, *J* = 8.4, 2.2 Hz, 1H), 7.93 (dd, *J* = 8.0, 2.0 Hz, 1H), 7.75–7.68 (m, 2H), 7.53 (d, *J* = 8.1 Hz, 1H), 7.28 (t, *J* = 7.4 Hz, 2H), 7.24–7.14 (m, 3H), 5.39–5.24 (m, 1H), 4.34–4.24 (m, 1H), 3.76 (d, *J* = 2.8 Hz, 1H), 3.56 (s, 2H), 3.52–3.46 (m, 8H), 3.22–3.08 (m, 4H), 2.77 (dd, *J* = 13.2, 6.5 Hz, 1H), 2.59 (s, 3H), 2.48–2.27 (m, 10H), 2.04–1.93 (m, 2H), 1.64–1.52 (m, 1H), 1.50–1.40 (m, 2H), 0.88–0.78 (m, 6H). ¹³C NMR (101 MHz, DMSO-*d*₆) δ 173.09, 172.36, 165.16, 151.50, 151.05, 144.19, 140.29, 138.63, 134.19, 133.50, 132.64, 132.54, 131.66, 131.00, 130.44, 130.11, 129.68, 128.65, 126.34, 123.97, 122.64, 117.73, 114.48, 112.24, 92.39, 88.75, 73.08, 70.07, 69.99, 69.37, 68.73, 57.94, 57.68, 56.05, 53.65, 53.31, 51.16, 41.60, 40.89, 39.04, 24.66, 23.55, 22.06, 20.93. HRMS (ESI) Calcd. for C₅₀H₆₀N₉O₆F₃ $[M+H]^+$,

940.4691; Found 1091.4675. HPLC purity = 95.91%, t_R 12.33 min.

4.2. Materials and methods of biological studies

4.2.1. Cells and reagents

K562, the leukemia cell lines, was purchased from the American Type Culture Collection (ATCC, Manassas, VA, USA). All cell lines including Ba/F3 cell lines were maintained in RPMI-1640 supplemented with 10% FBS, 100 U/mL penicillin, 50 mg/mL streptomycin, and 2 mmol/L glutamine in a humidified CO₂ incubator at 37 °C. CCK-8 was purchased from Dojindo Molecular Technologies Inc. (Kumamoto, Japan). Primary antibodies against c-Abl (2862S), GAPDH (2118) and anti-rabbit (7074S) or anti-mouse IgG horseradish peroxidase (HRP)-linked secondary antibodies were purchased from Cell Signaling Technology (Boston, MA, USA). All compounds were dissolved in DMSO (Sigma–Aldrich, St. Louis, MO, USA) at a concentration of 10 mmol/L and the solution was stored at –20 °C.

4.2.2. Stably transformed Ba/F3 cells

The Ba/F3 cell lines stably expressing Bcr-Abl^{T315I} were self-established. Using the mRNA of K562 cells (human chronic myeloid leukemia cells expressing the fusion protein Bcr-Abl) as a template, the full-length Bcr-Abl fusion gene was amplified by the method of molecular cloning and was loaded into the eukaryotic expression vector pCDNA3.1(+); then the plasmid pCDNA3.1(+) Bcr-Abl^{WT} expressing Bcr-Abl wild type was constructed. On the basis of this plasmid, a single point mutation primer was designed for targeting the T315I site, and *via* a site-directed mutation operation, the plasmid pCDNA3.1(+) Bcr-Abl^{T315I} was obtained. Ba/F3 cells transfected the pCDNA3.1(+) plasmids using Amaxa Cell Line Nucleofector Kit V (Lonza, Cologne, Germany) by electroporation. Stable lines were selected by G418 (Merck, Whitehouse Station, NJ, USA) and withdrawal of interleukin-3 (IL-3, R&D). The Ba/F3 stable cell lines were verified by monitoring both DNA sequences through DNA sequencing and protein expression levels of the corresponding T315I mutants through Western blotting analysis. Parental Ba/F3 cells were cultured in RPMI 1640 supplemented with 10% fetal bovine serum (FBS) and (IL-3, 10 ng/mL), while the Bcr-Abl^{T315I} transformed Ba/F3 stable cell lines were cultured in RPMI 1640 supplemented with 10% FBS without IL-3.

4.2.3. Western blot with degradation study

Cells were treated with various concentrations of each tested compound for a designated time. Then cells were lysed in using 1 × SDS sample lysis buffer (CST recommended) with protease and phosphatase inhibitors. Cell lysates were loaded and electrophoresed onto 8%–12% SDS-PAGE gel, then the separated proteins were transferred to a PVDF film. The film were blocked with 5% fat-free milk in TBS solution containing 0.5% Tween-20 for 2–4 h at rt, then incubated with the corresponding primary antibody (1:1000–1:800) overnight at 4 °C. After washing with TBST, HRP-conjugated secondary antibody was incubated for 2–4 h. The protein signals were visualized by ECL Western blotting detection kit (Thermo Scientific, Waltham, MA, USA), and detected with Amersham Imager 600 system (GE, Boston, MA, USA).

4.2.4. Co-immunoprecipitation

Cells were lysed by RIPA lysis buffer (#P0013D, Beyotime, China) with protease (#P1046-1, Beyotime) and phosphatase inhibitors (#P1046-2, Beyotime) on ice after treatment with various concentrations of **7o** for 24 h. Proteins were quantified using enhanced BCA protein assay kit (#P0009, Beyotime), and were adjusted to the same protein concentration using RIPA. About 4/5 of lysis buffer from different processed samples respectively were used for the Co-IP, the rest were used for the input. Protein of interest (CRBN) in the lysate is captured using a c-Abl antibody (#sc-23, Germany) and then the samples were incubated in 4 °C overnight. The processed cell lysates were added protein A+G agarose (#032019190322, Beyotime) at the second day, and precipitated along with its binding proteins for 2 h at 4 °C. After 2 h, beads in the cell lysates were washed using RIPA lysis buffer (#P0013D, Beyotime) without protease and phosphatase inhibitors for 5 times repeatedly. After a series of washes to remove non-bound proteins in the lysate, the resultant immune complexes are subjected to immunoblotting to determine the protein–protein interaction of interest.

4.2.5. Transferase-mediated deoxyuridine triphosphate-biotin nick end labeling (TUNEL) staining

Resected mouse tumors (ethics acceptance number: 20180226039) were fixed in 4% paraformaldehyde solution (Jingxin Biotech, China), then paraffin embedded and sectioned for TUNEL staining analysis according to the instructions of the manufacturer (11684817910, Roche, Germany).

4.2.6. Antiproliferation cell assay

Cells in the logarithmic phase were placed in 96-well plates (~3000 cells/well) in complete medium. After incubation overnight, the cells were exposed to the corresponding compounds or vehicle control at the indicated concentration for a further 72 h. Cell proliferation was evaluated by cell counting kit 8 (CCK8, CK04, Dojindo Laboratories, Kumamoto, Japan). OD₄₅₀ and OD₆₅₀ were determined by a microplate reader. Absorbance rate (A) for each well was calculated as OD₄₅₀–OD₆₅₀. The cell viability rate for each well was calculated as Eq. (1):

$$V(\%) = (A_s - A_c)/(A_b - A_c) \times 100 \quad (1)$$

and IC₅₀ values were further calculated by concentration–response curve fitting using GraphPad Prism 5.0 software. Each IC₅₀ value is expressed as mean ± SD. A_s is the absorbance rate of the test compound well, A_c is the absorbance rate of the well without either cell or test compound, and A_b is the absorbance rate of the well with cell and vehicle control.

4.2.7. Pharmacokinetics

Three male ICR mice of SPF weighing 18–25 g were prepared for intraperitoneal (i.p.) injection (ethics acceptance number: 20180226039). During the experiment, animals had free access to food, with the exception of specific fasting period. Dispensing method for intraperitoneal injection: the test compound is dissolved in a mixed solvent (5% DMSO+10% solutol+85% saline) at a concentration of 2 mg/mL. The compound was administered intravenously at a dose of 20 mg/kg. The time points of blood collection for intraperitoneal injection administration at 0.5, 1, 2, 4, 8, 12, 24, 36 and 48 h. The blood were taken *via* orbital venous plexus, 0.03 mL/time point. Samples were placed in tubes containing K2-EDTA and stored on ice until centrifuged. The blood

samples were centrifuged at 6800×g for 6 min at 2–8 °C within 1 h after collected and stored frozen at approximately –80 °C. The **7o** was analysed. The analytical results were confirmed using quality control samples for intra-assay variation. The accuracy of >66.7% of the quality control samples and 50% of all QC samples at each concentration level were between 80% and 120% of the known value(s). Standard set of parameters including area under the curve (AUC_{0–t} and AUC_{0–∞}), elimination half-life (t_{1/2}), maximum plasma concentration (C_{max}), time to reach maximum plasma concentration (T_{max}) were calculated using non-compartmental analysis modules in US Food and Drug Administration (FDA) certified pharmacokinetic program Phoenix WinNonlin 7.0 (Pharsight, USA) by the Study Director.

4.2.8. In vivo antitumor efficacy

Ba/F3 cells expressing Bcr-Abl^{T315I} were resuspended in normal saline (NS) solution and injected subcutaneously in the right flank of CB17-SCID mice (2 × 10⁶ cells/0.1 mL). At 5–7 days after inoculation, the status of proliferation of the Ba/F3 cells *in vivo* in mice was monitored by experimenters every day. Mice were then randomized to treatment groups when the mean tumor volume reached 100–200 mm³. Grouped mice were dosed once every two days through intraperitoneal injection for 14 consecutive days with **7o** of indicated doses, or vehicle (as described above). The body weight and tumor volume were monitored and recorded once every two days. Tumor volume was calculated as Eq. (2):

$$\text{Tumor volume} = L \times W^2/2 \quad (2)$$

where *L* and *W* are the length and width of the tumor, respectively. Resected mouse tumors were collected for H&E staining, IHC and WB analysis at the terminal experiment. The animal experiment was carried out under protocols approved by the Institutional Animal Care and Use Committee of the Medical College of Jinan University, Guangzhou, China.

Acknowledgments

This work was supported by National Natural Science Foundation of China (81922062 and 81874285), the National Key Research and Development Program of China (2018YFE0105800 and SQ2019YFE010401), National Science & Technology Major Project Key New Drug Creation and Manufacturing Program (2018ZX09711002-011-020, China), Guangdong Provincial Science and Technology Program (2018A050506043, China) and Jinan University.

Author contributions

Liang Jiang, Yuting Wang and Qian Li carried out the synthetic and some biology experiments. Zhengchao Tu and Sihua Zhu carried out the kinase inhibition assay. Sanfang Tu, Zhang Zhang and Ke Ding supervised the project. Xiaoyun Lu supervised the project, wrote and finalized the manuscript.

Conflicts of interest

The authors have no conflicts of interest to declare.

Appendix A. Supporting information

Supporting information to this article can be found online at <https://doi.org/10.1016/j.apsb.2020.11.009>.

References

1. Capdeville R, Buchdunger E, Zimmermann J, Matter A. Glivec (STI571, imatinib), a rationally developed, targeted anticancer drug. *Nat Rev Drug Discov* 2002;**1**:493–502.
2. Deininger M, Buchdunger E, Druker BJ. The development of imatinib as a therapeutic agent for chronic myeloid leukemia. *Blood* 2005;**105**:2640–53.
3. O'Hare T, Eide CA, Deininger MWN. Bcr-Abl kinase domain mutations, drug resistance, and the road to a cure for chronic myeloid leukemia. *Blood* 2007;**110**:2242–9.
4. Shah NP, Nicoll JM, Nagar B, Gorre ME, Paquette RL, Kuriyan J, et al. Multiple BCR-ABL kinase domain mutations confer polyclonal resistance to the tyrosine kinase inhibitor imatinib (STI571) in chronic phase and blast crisis chronic myeloid leukemia. *Canc Cell* 2002;**2**:117–25.
5. Kantarjian HM, Giles F, Gattermann N, Bhalla K, Alimena G, Palandri F, et al. Nilotinib (formerly AMN107), a highly selective BCR-ABL tyrosine kinase inhibitor, is effective in patients with Philadelphia chromosome-positive chronic myeloid leukemia in chronic phase following imatinib resistance and intolerance. *Blood* 2007;**110**:3540–6.
6. Quintascarda A, Kantarjian H, Dan J, Nicaise C, O'Brien S, Giles F, et al. Dasatinib (BMS-354825) is active in Philadelphia chromosome-positive chronic myeloid leukemia after imatinib and nilotinib (AMN107) therapy failure. *Blood* 2007;**109**:497–9.
7. Lu XY, Cai Q, Ding K. Recent developments in the third generation inhibitors of Bcr-Abl for overriding T315I mutation. *Curr Med Chem* 2011;**18**:2146–57.
8. O'Hare T, Shakespeare WC, Zhu X, Eide CA, Rivera VM, Wang F, et al. AP24534, a Pan-BCR-ABL inhibitor for chronic myeloid leukemia, potently inhibits the T315I mutant and overcomes mutation-based resistance. *Canc Cell* 2009;**16**:401–12.
9. Huang WS, Metcalf CA, Sundaramoorthi R, Wang Y, Zou D, Thomas RM, et al. Discovery of 3-[2-(imidazo[1,2-*b*]pyridazin-3-yl)ethynyl]-4-methyl-*N*-{4-[(4-methylpiperazin-1-yl)methyl]-3-(trifluoromethyl)phenyl}benzamide (AP24534), a potent, orally active pan-inhibitor of breakpoint cluster region-abelson (BCR-ABL) kinase including the T315I gatekeeper mutant. *J Med Chem* 2010;**53**:4701–19.
10. Massaro F, Molica M, Breccia M. Ponatinib: a review of efficacy and safety. *Curr Cancer Drug Targets* 2018;**18**:847–56.
11. Zabriskie MS, Eide CA, Tantravahi SK, Vellore NA, Estrada J, Nicolini FE, et al. BCR-ABL1 compound mutations combining key kinase domain positions confer clinical resistance to ponatinib in Ph chromosome-positive leukemia. *Canc Cell* 2014;**26**:428–42.
12. Braun TP, Eide CA, Druker BJ. Response and resistance to BCR-ABL1 targeted therapies. *Canc Cell* 2020;**37**:530–42.
13. Hamilton A, Helgason GV, Schemionek M, Zhang B, Myssina S, Allan EK, et al. Chronic myeloid leukemia stem cells are not dependent on Bcr. *Blood* 2012;**119**:1501–10.
14. Ichim CV. Kinase independent mechanisms of resistance of leukemia stem cells to tyrosine kinase inhibitors. *Stem Cells Trans Med* 2014;**3**:405–15.
15. Lai AC, Crews CM. Induced protein degradation: an emerging drug discovery paradigm. *Nat Rev Drug Discov* 2017;**16**:101–14.
16. Ottis P, Crews CM. Proteolysis targeting chimeras: induced protein degradation as a therapeutic strategy. *ACS Chem Biol* 2017;**12**:892–8.
17. Schneekloth AR, Pucheault M, Tae HS, Crews CM. Targeted intracellular protein degradation induced by a small molecule: en route to chemical proteomics. *Bioorg Med Chem Lett* 2008;**18**:5904–8.
18. Winter GE, Buckley DL, Paulk J, Roberts JM, Souza A, Dhe-Paganon S, et al. Drug development. Phthalimide conjugation as a strategy for *in vivo* target protein degradation. *Science* 2015;**348**:1376–81.
19. Bondeson DP, Mares A, Smith IED, Ko E, Campos S, Miah AH, et al. Catalytic *in vivo* protein knockdown by small-molecule PROTACs. *Nat Chem Biol* 2015;**11**:611–7.
20. Tan L, Gray NS. When kinases meet PROTACs. *Chin J Chem* 2018;**36**:971–7.
21. Wang Y, Jiang X, Feng F, Liu W, Sun H, et al. Degradation of proteins by PROTACs and other strategies. *Acta Pharm Sin B* 2020;**10**:207–38.
22. Lai AC, Toure M, Hellerschmied D, Salami J, Jaime-Figueroa S, Ko E, et al. Modular PROTAC design for the degradation of oncogenic BCR-ABL. *Angew Chem Int Ed* 2016;**55**:807–10.
23. Demizu Y, Shibata N, Hattori T, Ohoka N, Motoi H, Misawa T, et al. Development of BCR-ABL degradation inducers via the conjugation of an imatinib derivative and a cIAP1 ligand. *Bioorg Med Chem Lett* 2016;**26**:4865–9.
24. Shimokawa K, Shibata N, Sameshima T, Miyamoto N, Ujikawa O, Nara H, et al. Targeting the allosteric site of oncoprotein BCR-ABL as an alternative strategy for effective target protein degradation. *ACS Med Chem Lett* 2017;**8**:1042–7.
25. Zhao Q, Ren C, Liu L, Chen J, Shao Y, Sun N, et al. Discovery of SIAIS178 as an effective BCR-ABL degrader by recruiting Von Hippel-Lindau (VHL) E3 ubiquitin ligase. *J Med Chem* 2019;**62**:9281–98.
26. Yang Y, Gao H, Sun X, Sun Y, Qiu Y, Weng Q, et al. Global PROTAC toolbox for degrading BCR-ABL overcomes drug-resistant mutants and adverse effects. *J Med Chem* 2020;**63**:8567–83.
27. Ren X, Pan X, Zhang Z, Wang D, Lu X, Li Y, et al. Identification of GZD824 as an orally bioavailable inhibitor that targets phosphorylated and nonphosphorylated breakpoint cluster region-abelson (Bcr-Abl) kinase and overcomes clinically acquired mutation-induced resistance against imatinib. *J Med Chem* 2013;**56**:879–94.
28. Gustafson JL, Neklesa TK, Cox CS, Roth AG, Buckley DL, Tae HS, et al. Small-molecule-mediated degradation of the androgen receptor through hydrophobic tagging. *Angew Chem Int Ed* 2015;**54**:9659–62.
29. Shibata N, Miyamoto N, Nagai K, Shimokawa K, Sameshima T, Ohoka N, et al. Development of protein degradation inducers of oncogenic BCR-ABL protein by conjugation of ABL kinase inhibitors and IAP ligands. *Canc Sci* 2017;**108**:1657–66.